Impact of Carbon Source Supplementations on Pseudomonas aeruginosa Physiology

Salomé Sauvage, Charlotte Gaviard, Ali Tahrioui, Laurent Coquet, Hung Le, Stéphane Alexandre, Ahmed Ben Abdelkrim, Emeline Bouffartigues, Olivier Lesouhaitier, Sylvie Chevalier, et al.

Impact of carbon source supplementations on *Pseudomonas aeruginosa* physiology

Salomé Sauvage[1,2], Charlotte Gaviard[1,2], Ali Tahrioui[3], Laurent Coquet[1,2], Hung Le[1], Stéphane Alexandre[1], Ahmed Ben Abdelkrim[4], Emeline Bouffartigues[3], Olivier Lesouhaitier[3], Sylvie Chevalier[3], Thierry Jouenne[1,2], and Julie Hardouin[1,2,]*

[1] Normandie Université, UNIROUEN, INSA, CNRS Polymers, Biopolymers, Surface Laboratory, 76821 Mont-Saint-Aignan cedex, France

[2] PISSARO Proteomic Facility, IRIB, 76820 Mont-Saint-Aignan, France

[3] Laboratoire de microbiologie signaux et microenvironnement, LMSM EA4312, 55 rue Saint-Germain, 27000 Evreux, France

[4] Lactanet, Valacta, 555 Boul des Anciens-Combattants, Sainte-Anne-de-Bellevue, QC H9X 3R4, Canada

Keywords: *Pseudomonas aeruginosa*, carbon sources, virulence, antibiotic resistance, biofilm, physiological changes

Abstract

Pseudomonas aeruginosa is an opportunistic pathogen highly resistant to a wide range of antimicrobial agents, making its infections very difficult to treat. Since microorganisms need to perpetually adapt to their surrounding environment, understanding the effect of carbon sources on *P. aeruginosa* physiology is therefore essential to avoid increasing drug-resistance and better fight this pathogen. By a global proteomic approach and phenotypic assays, we investigated the impact of various carbon source supplementations (glucose, glutamate, succinate and citrate) on the physiology *P. aeruginosa* PA14 strain. A total of 581 proteins were identified as differentially expressed in the 4 conditions. Most of them were more abundant in citrate supplementation and were involved in virulence, motility, biofilm development and antibiotic resistance. Phenotypic assays were performed to check these hypotheses. By coupling all this data, we highlight the importance of the environment in which the bacterium evolves on its metabolism, and thus the necessity to better understanding metabolic pathways implied in its adaptative response according to the nutrients availability.

Introduction

Microorganisms need to perpetually adapt to their surrounding environment. They first rapidly assimilate their favorite carbon source and then use appropriate metabolic pathways to assimilate other non-preferential carbon sources present in the environment, necessary for their survival [1].

It is well known that carbon sources may have a significant impact on the metabolism of microorganisms. For example, the use of alternative carbon sources to glucose makes the yeast *Saccharomyces cerevisiae* more resistant to stresses [2]. In the presence of glucose or lactate, *Candida albicans* shows an alteration of its cell wall structure, antifungal drug resistance and virulence [1]. In *Pseudomonas putida* and *Acinetobacter baylyi*, succinate has an inhibiting effect on the degradation of hydrocarbons and aromatic compounds [3]. This carbon source also leads to the repression of catabolites for the use of non-preferential carbon sources such as glucose in *Pseudomonas fluorescens* [4].

Carbon sources can thus impact important mechanisms such as bacterial virulence, biofilm formation or antibiotic resistance. Indeed, to regulate their intracellular lifestyle, including their metabolism, pathogens need to secrete virulence factors to get nutrients available in their environment [5-7]. Hence, pathogenesis and virulence of various bacterial species can be modified according to the activation or not of the glyoxylate cycle [6, 8]. Biofilm formation can also be altered by the carbon source availability [9]. Biofilm development is allowed by flagella and type IV pili, which play a role in the irreversible attachment to surface, an important step in biofilm development [10]. In *P. fluorescens*, citrate or glutamate supplementation in minimal medium restored the ability of non-motile mutants to form biofilms [11]. Moreover, motility studies on *P. aeruginosa* have mainly focused on its swarming motility, which is involved in the development of biofilms. This type of motility requires flagella, rhamnolipid biosurfactants, specific cell density and availability of some carbon sources [12]. Shrout *et al*. showed that the carbon

source impacts the swarming motility of *P. aeruginosa*, as well as its control by the *quorum sensing* (*QS*) [13]. Recently, we have shown that the number of acetylated and succinylated proteins in *P. aeruginosa* was significantly dependent of the carbon sources. Modified proteins are more numerous when bacteria were grown in citrate-supplemented culture media than in glucose, succinate or glutamate-supplemented media [14]. It is interesting to note, that several of these modified proteins were involved in virulence, antibiotic resistance, or biofilm formation, highlighting the role of carbon sources in the *P. aeruginosa* physiology.

P. aeruginosa is a Gram-negative bacterium classified as Priority 1 by the World Health Organization for which it is urgent to find new treatments [15]. Indeed, this human opportunistic pathogen is the most associated with hospital-acquired diseases and predominantly affects patients with cystic fibrosis [16]. It is able to bypass host innate immunity and is highly resistant to a wide range of antimicrobial agents [17], making its infections very difficult to treat [16]. In the aim to explore new strategies to fight against virulence and resistance of bacteria, understanding the impact of carbon sources on the bacterial physiology is therefore an interesting avenue. A better knowledge of the relationship between metabolism and pathogenesis is indeed essential to avoid increasing drug-resistance and virulence of bacteria [18-23].

In the present study, using a quantitative proteomic approach, we investigated the impact of different growth media (supplementation of glucose, citrate, succinate, or glutamate) on protein expression and highlighted 581 proteins differentially expressed. Interestingly, the citrate condition was clearly stand out from the other conditions, since many of the accumulated proteins were involved in virulence, antibiotic resistance, or biofilm formation. We made the relation of this expression with several phenotypes as virulence, antibiotic resistance, biofilm formation, or motility *of P. aeruginosa* PA14 strain. All these results pointed out that, in the presence of citrate, *P. aeruginosa* implements specific pathways to survive and adapt to its environment, modifying its global virulence.

Materials and methods

1. Bacterial strains, media and growth conditions

The strain used in this study is *P. aeruginosa* PA14 strain obtained from the laboratory of Dr Ausubel (Massachusetts General Hospital). An overnight culture of *P. aeruginosa* PA14 grown in Mueller Hinton Broth (MHB, Difco) diluted at a final concentration of 10^7 CFU/mL was used to inoculate a controlled liquid medium (CLM) (90 mM Tris-HCl, 4 mM Tris-base, 9 mM NH_4Cl, 0.45 mM $CaCl_2$, 0.2 mM $MgSO_4$, 18 µM $MnSO_4$, 18 µM $FeSO_4$, 0.2% yeast extract) supplemented with glucose (CLM-glucose), glutamate (CLM-glutamate), succinate (CLM-succinate) or citrate (CLM-citrate) at a final concentration of 80 mM. Cultures were then grown at 37 °C under constant shaking at 140 rpm for 24 hours.

2. Quantitative proteomic analysis

2.1. Protein extraction

Intra- and extra-cellular protein extractions were performed as previously described [14, 24]. Briefly, cultures of *P. aeruginosa* PA14, grown in CLM-glucose, -glutamate, -succinate or -citrate during 24 hours, were centrifuged (9,000 g, 25 min, 4 °C). First, the bacterial pellet was resuspended in 10 mL of Tris-HCl buffer 20 mM (pH 7.4) supplemented with a protease inhibitor cocktail (10 µL/mL, Protease Inhibitor Cocktail-Bacterial, Sigma-Aldrich). The mixture was freeze-thawed for three cycles and then sonicated on ice six times, each for 1 min. The lysate was centrifuged at 9,000 g for 25 minutes at 4 °C. An ultracentrifugation was applied to the supernatants (60,000 g, 45 min, 4 °C) to separate cytoplasmic (soluble) and membrane proteins.

The culture supernatant which contained extracellular proteins was filtered through 0.22 µm filters (GSWP 47 mm, Millipore) and precipitated with 17.5% (w/v) trichloroacetic acid (TCA) (Thermo Fisher Scientific) overnight at 4 °C. The protein pellet was centrifuged (8,900g, 25

min, 4 °C) and then washed with acetone (8,900g, 25 min, 4 °C). Proteins were then solubilized in R2D2 denaturing buffer (7 M urea, 2 M thiourea, Tri-N-butylphosphine (TBP) 2 mM, dithiothreitol (DTT) 20 mM, 0.5% (w/v) 3-(4-heptyl)phenyl-3-hydroxypropyl)dimethylammoniopropanesulfonate (C7BzO), 2% (w/v) 3-[(3-cholamidopropyl)dimethylammonio]-1-propanesulfonate hydrate (CHAPS)).

Intra- and extra-cellular protein concentrations were evaluated by Bradford analysis (Bio-Rad). Samples were stored in aliquots at -20 °C until further use.

2.2. Protein digestion

Twenty-five micrograms of proteins were mixed with sodium dodecyl sulfate (SDS) loading buffer (62 mM Tris-HCl pH 6.8, 20% glycerol (v / v), 0.04% bromophenol blue (w / v), 0.1 M DTT, SDS 4% (w / v)) then loaded onto a SDS-PAGE stacking gel 7%. A short electrophoresis was performed (10 mA, 15 min) to concentrate proteins. After migration, gels were stained with Coomassie Blue G250 and destained with 50% ethanol (v/v) and 10% acetic acid (v/v). The revealed protein band was excised and washed three times with water. Cysteines were alkylated with 15 mM iodoacetamide, 30 minutes in the dark. Gel bands were treated with 50% acetonitrile (ACN)/50% ammonium bicarbonate 10 mM, pH 8 (2 times, 5 min) and dried with 100% ACN (3 times, 10 min). Then proteins were digested with trypsin (1 µg per band), overnight at 37 °C, in ammonium bicarbonate 10 mM, pH 8. Peptide were extracted with 100% ACN (3 times, 10 min) and then dried. For each carbon sources growth conditions, four biological replicates were carried.

2.3. NanoLC-MS/MS protein analyses with Q Exative Plus

After digestion of intra- and extra-cellular proteins, peptides were solubilized in 0.1% formic acid (FA) (v/v) and analyzed on Q Exactive Plus (Thermo Scientific) equipped with a nanoESI

source. Peptides were injected onto an enrichment column (C18 Pepmap100 precolumn (300 µm ID × 5 mm, 5 µm, 100 Å), Thermo Scientific). The separation was carried out using a PepMap^{TM} RSLC C18 (Thermo Scientific). The buffers for the mobile phase were composed of 100% H_2O/0.1% FA (A) and 80% ACN/20% H_2O/0.1% FA (B). The elution gradient duration was 120 minutes: 2 to 35% B from 0 to 84 minutes, 35 to 90% B from 84 to 94 minutes, 90% B from 94 to 99 minutes, and 2% B from 100 to 120 minutes. The flow rate was 300 µL/min. The temperature of the column was set at 40 °C. The maximum injection time was set to 100 ms. The capillary voltage was 1.6 kV. The temperature of the capillary was 275 °C. The analysis was performed in HCD mode. The *m/z* detection range is 400-1,800. The resolution was 70,000 in MS, and 17,500 in MS/MS. The 10 most intense ions (Top 10) were selected and then fragmented. Nitrogen was used as a collision gas. Fragmentation occurred with normalized collision energy of 27. All spectra obtained were exported in ".raw" format to identify peptides and proteins with Proteome Discoverer 1.4 software (Thermo Scientific).

2.4. Protein quantification

The peptides were analyzed by nano liquid chromatography coupled with mass spectrometry (LC-MS/MS) by direct analysis, with the Q-exactive Plus mass spectrometer. Raw data were imported in Progenesis LC-MS/MS software (Waters, version 4.1, Newcastle, UK). A 2-dimensional map was generated for each sample (retention time versus *m/z* ratio). The spots present on the 20 2D maps were then aligned. Mono-charged ions and those with a charge greater than 5 are excluded from the analysis. After alignment and normalization, statistical analysis was performed for one-way analysis of variance (ANOVA) calculations. Peptide features presenting p-value and q-value less than 0.05, and a power greater than 0.8 were retained to achieve a principal component analysis (PCA). MS/MS spectra from selected peptides were exported

for peptide identification with Mascot (Matrix Science, version 2.2.04) against the *P. aeruginosa* PA14 database available online (https://www.*pseudomonas*.com/downloads/sequences) [25]. Database searches were performed with the following parameters: 1 missed trypsin cleavage site allowed; variable modifications: carbamidomethylation of cysteine and oxidation of methionine. Mass tolerances for precursor and fragment ions were both set at 5 ppm. Then, Mascot search results were imported into Progenesis. Peptides with an identification score greater than 20 are retained. Proteins identified with less than 3 peptides were discarded. For each growth condition, the total cumulative abundance of the protein was calculated by summing the abundances of peptides. The software compared the intensity of the isotopic mass of all the ions for each carbon source. The abundances were normalized to perform a relative quantification of each protein within the 4 conditions. To keep only the proteins exhibiting a differentially significant expression, new statistical filters were applied at the protein level: p-value <0.05, q-value <0.05, power> 0.8 and with a fold-change ≥ 2. The MS proteomics data have been deposited to the ProteomeXchange Consortium via the PRIDE partner repository with the dataset identifier PXD030421 [Username : reviewer_pxd030421@ebi.ac.uk ; Password: k2LMmWsR].

2.5. Statistical analysis

To compare protein expression variations between the 4 conditions, a one-way analysis of variance (ANOVA) test with post hoc pairwise was used. The univariate associations between selected proteins and the different groups were assessed by simple regression. Additionally, a principal coordinate analysis (PCoA) was conducted, to visualize the relationships among groups at each stage (Figure S1A). Proteins with a similar expression pattern were presented as heat map. Proteins with the same expression variation were grouped, showing strong correlation. Relationships between the marker proteins were visualized with a correlation matrix with

corrplots (Pearson's r correlation coefficient) [26]. Hierarchical clustering of each growth condition was performed using Euclidean distance metric and Average linkage method (unsupervised clustering). All data processing and statistical analysis were performed using R 4.1 [27].

3. Quantification of *QS* molecules

3.1. Extraction of *QS* molecules

P. aeruginosa PA14 was grown in CLM-glucose, -glutamate, -succinate or -citrate during 24 hours. For *QS* molecules extraction from supernatants, cultures were centrifuged and the supernatants were collected and filtered. For *QS* molecules extraction from cells, bacterial pellets were collected by centrifugation, washed twice with CLM. One hundred percent of methanol was then added to the pellets to allow lysis. After centrifugation, the supernatants were filtered to remove all cell debris.

The supernatant and cell samples were then supplemented with deuterated 4-hydroxy-2-heptylquinoline (HHQ-D4) and *Pseudomonas* quinolone signal (PQS-D4) provided by the laboratory of Pr Déziel (Institut National de la Recherche Scientifique, Institut Armand Frappier, Canada), and then extracted twice with equal volume of acidified ethyl acetate (glacial acetic acid 0.01% v/v in ethyl acetate). The organic layers were collected and evaporate. The supernatant and cell extracts were then stored at -20 °C until use.

3.2. Detection of *QS* molecules by HPLC-MS/MS

Extracts were re-suspended in 100 µL of 50% ACN, 0.1% FA in water, sonicated twice for 15 minutes, and then centrifuged for 10 minutes at 7,000 g. Appropriated volumes of supernatant were carefully transferred to vials for HPLC (high performance liquid chromatography)-MS/MS and *N*-heptanoyl-L-homoserine lactone (C_7-HSL) was added in all samples at 250 pg/µL final concentration.

Separation of the biomolecules was performed with an Agilent 1290 Infinity II HPLC system coupled to a 6545XT AdvanceBio Q-TOF mass spectrometer (Agilent Technologies, USA). The column was a Zorbax Eclipse Plus C18, 2.1 mm x 100 mm with 1.8 µm particle size (Agilent Technologies, USA). The buffers for the mobile phases were 0.1% FA in water (A) and 90% ACN, 0.1% FA in water (B). The constant flow rate was 0.4 mL/min and the column temperature was settled at 60 °C. The elution gradient duration was 18 min: 3 to 10% B for 3 min, 10 to 45% B for 1 min, 45 to 75% B for 1 min, 75 to 90 %B for 3.5 min, a flushing phase at 90% B for 4 min and a re-equilibration phase at 3% B for 5.5 min. The volume of diluted samples injected onto the column was 1 µL. The mass spectrometer operated in positive electrospray ionization mode and in full scan. The settings were: Drying Gas: 12 L/min, Nebulizer: 60 psi, Sheath Gas Temperature: 200 °C, Sheath Gas Flow: 11 L/min, Capillary Voltage: 3,500 V and Skimmer: 65 V. The gas temperature of ESI source and the MS-TOF fragmentor voltage were fixed at 150 °C and 100 V, respectively, in the aim to improve the detection sensitivity of biomolecules. Moreover, "fragile ions" mode was activated on the instrument. The m/z value was scanned from 50 to 950 in MS and MS/MS modes and collected at a rate of 2 spectra/s with a maximum of 5 precursors for fragmentation in MS/MS with collision energies of 5, 10, 15, 20, 25 and 30 V.

The MS data analysis was carried out with the Agilent MassHunter software (B.07.00 version). *N*-butanoyl-homoserine lactone (C_4-HSL), *N*-(3-oxododecanoyl)-L-homoserine lactone (3-oxo-C_{12}-HSL), HHQ and PQS were detected at [M+H+] m/z of 172.09, 298.20, 244.16 and 260.16, respectively, with m/z values varying from ± 0.02 Da. For each biomolecule, the retention times of Extracted-Ion Chromatogram (EIC)-peaks were compared to those of standard molecules provided by Sigma-Aldrich for C_4-HSL (reference: 09945) and 3-oxo-C_{12}-HSL (reference: 09139). The identifications were confirmed by the presence of specific ion fragments

from MS2 spectra such as the lactone-ring ion (m/z = 102.055) for the AHL molecules or the cyclic moiety ion for HHQ and PQS (Figure S2).

3.3. Identification and quantification of *QS* molecules by HPLC-MS/MS

The area of each EIC-peak, corresponding to the relative abundance of $[M+H^+]$ ions detected on MS spectra, was measured. Only areas with values included in the linear calibration curves previously established with standard molecules (Figure S3) were retained for the quantification.

C_4-HSL and 3-oxo-C_{12}-HSL were quantified using C_7-HSL as standard since this AHL is not naturally produced by bacteria. The amount of AHLs in the samples was determined by reporting the ratio [C_4 or C_{12}/C_7 peak area] on a calibration curve (Figure S4).

Quantifications of PQS and HHQ were performed by measuring the relative areas of the EIC peaks for corresponding ions and for internal standard ions (PQS-D4 and HHQ-D4). Then, the ratio [biomolecule peak area / internal standard peak area] was multiplied by the concentration of the internal standards added during extraction protocol.

4. Quantification of rhamnolipids

4.1. Extraction of rhamnolipids

Twenty-four hours cultures of *P. aeruginosa* PA14 grown in CML-glucose, -glutamate, -succinate or -citrate supplementation were centrifuged (10,000 g, 10 min, 4 °C) and the resulting supernatants were filtered through a 0.22 µm syringue filter (Millex-GP, Merck Millipore Ltd, Ireland). The sterilized supernatant was next adjusted to pH=3 with HCl 1M. The rhamnolipids were extracted from 10 mL acidified supernatants with the same volume of ethyl acetate. A phase of vigorously mixture for 10 minutes followed by a centrifugation (4,000 g, 10 min, 20 °C) were carried out twice. The solvent containing the rhamnolipids was then collected and evaporated under a chemical hood before to be stored at -20 °C.

4.2. Detection of rhamnolipids by HPLC-MS/MS

The dry rhamnolipid extracts were solubilized in 200 µL 50% ACN/50% H_2O and then diluted in 30% ACN/70% H_20 supplemented with 4 mM ammonium acetate for HPLC-MS/MS analyses. The same HPLC-MSMS coupling system as previously described above for AHLs analyses was used. The separation by reverse-phase HPLC was carried out with a Zorbax SB-C18 column (4.6 mm x 150 mm, 3.5 µM particle size, Agilent, USA). The mobile phases were H_20 for solvent A and 90% ACN/10% H_2O for solvent B with 4 mM ammonium acetate in both. The chromatographic separation was performed for 20 minutes at 50 °C with a flow rate of 0.750 mL/min. The elution gradient consisted of a first step of 3 minutes at 35% B followed by a linear gradient from 40% to 90% B for 13 minutes, 90% B for 2 minutes, a short phase of few seconds from 90% to 40% B and 40% B for 2 minutes. One µL of diluted rhamnolipid extracts were injected. LC-MS/MS Q-Tof was performed in negative mode with an ion detection on a mass range of 50-1500 m/z. Two spectra/s were set up for MS. The collision energy for fragmentation in MS2 was from 5 to 25 V. The parameters were 200 °C for the gas temperature in source, 3.5 kV and 175 V for the capillary and fragmentor voltage respectively. The rhamnolipids were detected by extracting from MS spectra the EIC peaks of expected [M-H-] m/z for each mono-di-rhamno mono-di-lipids (Figure S5).

4.3. Identification and quantification of rhamnolipids by HPLC-MS/MS

The identifications were confirmed by analysis of the MS2 spectra resulting from the fragmentation of MS ions suspected to be biosurfactants according their m/z masses. The MS2 ions resulted mainly of fragmentation between the two fatty acid chains and, with lower abundance, between the rhamnose and the first fatty acid chain. For quantification, the values of EIC peak areas were reported on a linear calibration curve established with commercial rhamnolipids (R95MD, Sigma) (Figure S6).

5. Growth curves

P. aeruginosa PA14 growth in CLM-glucose, -glutamate, -succinate or -citrate was monitored at 37 °C over the course of 24 hours using the Spark 20M multimode Microplate Reader, equipped with an active temperature regulation system (Te-CoolTM, Tecan Group Ltd., Männedorf, Switzerland). An initial bacterial inoculum of 10^7 CFU/mL was used. Absorbance at 545 nm was recorded every 30 minutes. The bacterial growth curves were determined by plotting the values against time.

6. Motility assays

To assess swarming, or twitching motilities, 1 or 2% of technical agar (Difco) were used, respectively, and 0.4% of noble agar (Difco) for swimming. Plates were inoculated from 24-hours culture of *P. aeruginosa* in CLM-glucose, -glutamate, -succinate or -citrate, and incubated at 37 °C overnight for swimming, and 36 hours for twitching and swarming. For swimming and swarming, the diameter (mm) of the circular zone of growth was measured and expressed as a mean value (n=3). For twitching assay, the agar was removed and the plate was stained with 0.4% crystal violet (CV) during 15 minutes. Next, the CV was removed, the plate was washed with ultrapure water and the halo formed was measured and its diameter (mm) expressed as a mean value (n=3).

7. Biofilm quantification assay

A 96-well plate was inoculated with *P. aeruginosa* PA14, from 24-hours culture in CLM-glucose, -glutamate, -succinate or -citrate, and incubated at 37 °C during 24 hours. Then, the plate was rinsed twice with ultrapure water and stained with 0.1% CV for 10 minutes. Next, the CV was removed by pipetting and the wells were rinsed slowly three times with ultrapure water.

When the plate was dried, EtOH 30% was added and the OD at 595 nm was measured in a VICTOR3 plate reader (Perkin-Elmer).

8. Fluorescence anisotropy assay

Twenty-four-hours-old cultures of *P. aeruginosa* PA14 performed in CLM-glucose, -glutamate, -succinate or -citrate were centrifuged for 5 minutes at 7,500 g. The bacterial pellets were washed twice with 10 mM $MgSO_4$ solution. Next, bacterial suspensions adjusted at 0.1 of $OD_{580\ nm}$ in the same solution were labelled with 1,6-diphenyl-1,3,5-hexatriene (DPH) at 4 mM. The samples were then incubated for 30 minutes in the dark. Finally, the fluorescence polarization measurements were performed using a Spark 20M multimode Microplate Reader, equipped with an active temperature regulation system (Te-CoolTM, Tecan Group Ltd.). Excitation and emission wavelengths were set to 365 nm and 425 nm, respectively, and the fluorescence anisotropy (FAn) was calculated according to Lakowicz [28]. Three measurements were performed for each sample and data were recorded using SparkControlTM software (Version 2.1, Tecan Group Ltd.). The correlation between fluorescence polarization and membrane fluidity is an inverse one, where increasing anisotropy values correspond to a more rigid membrane and vice versa. All values are reported as means of triplicate analyses for each experimental variable.

9. Minimum inhibitory concentration determination

One hundred µL of a *P. aeruginosa* PA14 culture corresponding to 10^6 CFU/mL, performed in CLM-glucose, -glutamate, -succinate or -citrate during 24 hours, were used to inoculate 100 µL of CLM-glucose, -glutamate, -succinate or -citrate containing increasing concentrations of antibiotics (0.125 to 64 µg/mL for ticarcillin, tetracycline, tobramycin, gentamycin, ceftazidime and imipenem, 0.007 to 4 µg/mL for ciprofloxacin, and 0.007 to 4 µg/mL for CLM-glucose, 0.125 to 64 µg/mL for CLM-glutamate and CLM-succinate, and 8 to 4096 µg/mL for CLM-

citrate for colistin). After 24 hours of incubation at 37 °C under constant shaking at 140 rpm, the minimum inhibitory concentrations (MICs) of antibiotics were determined by measuring the OD at 550 nm in a VICTOR3 plate reader (Perkin-Elmer).

10. Zeta potential of bacteria in presence of colistin

One mL of a 24-hours-old culture of *P. aeruginosa* PA14, grown in CML-glucose, -glutamate, -succinate or -citrate, (cell concentration: 10^7 CFU/mL) before to be treated with 100 µg/mL of colistin during 20 minutes under shaking in the dark, before to be centrifugated (5,000 rpm, 2 min, 20 °C). The pellet was then washed with ultrapure water (5,000 rpm, 2 min, 20 °C). Next, bacteria were resuspended in to reach 10^7 CFU/mL in the capillary. Zeta potential measurements were performed using the Zetasizer Nano ZS (Malvern Instruments Ltd, UK) at 25 °C and data were analyzed using Malvern's Zetasizer Software version 7.11.

11. Pyocyanin quantification assay

Supernatants from 24-hours-old cultures of *P. aeruginosa* PA14, grown in CLM-glucose, -glutamate, -succinate or -citrate, were collected by centrifugation. Pyocyanin was extracted with one volume of chloroform. The chloroform layer (blue layer) was acidified by adding ½ volume of 0.5 M HCl. The absorbance of the HCl layer (pink layer) was recorded at 520 nm using the Spark 20M multimode Microplate Reader controlled by SparkControlTM software Version 2.1 (Tecan Group Ltd.). The data were normalized for bacterial cell density ($OD_{545\ nm}$).

12. Virulence towards human lung A549 cells

Human lung A549 cells were cultured in Dulbecco's Modified Eagle's Medium (DMEM, Lonza, BioWhittaker®) supplemented with 4.5 g/L glucose, L-glutamine, 10% heat-inactivated

(30 min, 56 ºC) fetal bovine serum, and 100 Units/mL each of penicillin and streptomycin antibiotics. Cells were grown at 37 ºC under an atmosphere of 5% CO_2 and 95% air with regularly medium change until a confluent monolayer was obtained. The virulence of *P. aeruginosa* PA14 cells grown in CLM-glucose, -glutamate, -succinate or -citrate was determined using an enzymatic assay (PierceTM LDH Cytotoxicity Assay Kit, Thermo ScientificTM), which measures lactate dehydrogenase (LDH) released from the cytosol of damaged A549 cells into the supernatant. After 5 and 6 hours of incubation with *P. aeruginosa* PA14 (initial cell concentration of 10^6 CFU/mL) grown in CLM-glucose, -glutamate, -succinate or -citrate, the supernatants from confluent A549 monolayers grown on 24-well tissue culture plates were collected and the concentration of the LDH release was quantified. A549 cells exposed to 1X Lysis Buffer were used as a positive control of maximal LDH release (100% lysis) as specified by the manufacturer's recommendations. The background level (0% LDH release) was determined with serum free culture medium.

13. Confocal Laser Scanning Microscopy (CLSM)

Biofilm formation at the solid-liquid interface was achieved in glass coverslips as previously described [29]. Briefly, aliquots of 1 mL from 24-hours culture of *P. aeruginosa* PA14 grown in CLM-glucose, -glutamate, -succinate or -citrate at 10^7 CFU/mL were transferred into each well (24-well flat-bottomed plate) containing a glass coverslip ø12 mm. The plate was incubated at 37 °C without shaking in the dark for 24 hours. The medium was then discarded, and the biofilms were washed twice with 0.01 M phosphate buffered saline (PBS). Biofilms were finally stained with Syto9 and Hexidium Iodide (Thermo Fisher Scientific, MA, USA) for 30 minutes following the manufacturer's protocol prior to microscopy.

14. Atomic force microscopy (AFM)

14.1. Planktonic samples preparation

One mL of a *P. aeruginosa* PA14 suspension (OD_{600nm} between 0.5 and 1.0), from an overnight culture in CLM-glucose, -glutamate, -succinate or -citrate at 37 °C under constant shaking at 140 rpm, was centrifuged (2,000 g, 5 min, 20 °C). Cell pellet was washed with ultrapure water (2,000 g, 5 min, 20 °C), resuspended in 500 µL of ultrapure water, and 10 µL of bacterial solution were apply onto a mica slide enclosed in gelatin. After 10 minutes of drying, mica slides were washed once with 0.01 M PBS and twice with ultrapure water. Samples were then dried in vacuum cabinet during 4 hours before to be observed by atomic force microscopy (AFM).

14.2. Biofilm samples preparation

Glass discs were inoculated with 1 mL of a *P. aeruginosa* suspension at 10^7 CFU/mL, from an overnight culture in CLM-glucose, -glutamate, -succinate or -citrate at 37 °C under constant shaking at 140 rpm. Discs were incubated at 37 °C in the dark during 6 hours, and then washed one time with 0.01 M PBS solution and twice with ultrapure water. Discs were dried in a vacuum cabinet overnight before to be observed in AFM.

14.3. Observation by AFM

AFM imaging was performed using a Nanoscope 8 Multimode microscope (Bruker Nano Surfaces, Santa Barbara, CA, USA). For each sample, a 100 µm piezoelectric scanner was used. Imaging was achieved in the air either using the contact mode (biofilm samples) or using the PeakForce® mode (planktonic samples). In the contact mode, the cantilevers used were characterized by a low spring constant of about 0.06 N/m and were equipped with a sharpened silicon nitride tip (DNP-S, Bruker). All the measurements were performed with the feedback loop on

(constant force from 10-9 to 10-8 N). For the PeakForce® mode imaging, a silicon nitride cantilever with a spring constant of about 0.4 N/m and a silicon tip was used (ScanAsyst-Air, Bruker). Images were obtained with a PeakForce Tapping frequency of 2 kHz with the auto-amplitude on.

All images are presented in the height mode and are topview images. Flatten and three points levelling operations were usually done using the Gwyddion AFM software (http://gwyddion.net/). In addition, images were processed using a local contrast filter (kernel size 2 px, blending depth 2, and weight 1) in order to visualize the bacteria surface. Then, the local contrast image was overlayed to the topographic image using the GIMP software (https://www.gimp.org/downloads/) in order to get a more meaningful image.

15. Extraction of RNA and analyses by qRT-PCR

Synthesis of cDNAs and real time PCR were performed as previously described (Supplementary Data S1) [30], using primers described in Supplementary Table S1. PCR reactions were performed in biological triplicate and technical duplicate (except for the citrate carbon source) with the 7300 Real Time PCR System apparatus (Applied Biosystems). The 300 mM reactions contained 2X SYBR Green PCR Master Mix (including AmpliTaq Gold DNA Polymerase, Applied Biosystems), 10 µM of each primer, and cDNAs diluted to one tenth. The experimental conditions were 95 °C for 10 minutes for polymerase activation, and 40 cycles at 95 and 60 °C for 60 and 30 seconds, respectively. ROX dye was used as passive reference to normalize for non-PCR related fluorescence variations. The mRNAs amount was calculated by comparing the threshold cycles (Ct) of target genes with those of control sample groups and the relative quantification of the mRNAs of interest was obtained by the comparative Ct ($2^{-\Delta\Delta Ct}$) method using DataAssist™ software (Applied Biosystems) with *rpoS* and *nadB* as endogenous control. ΔCt values were calculated by subtracting the *rpoS* and *nadB* Ct value of a sample from the Ct

value of an mRNA of interest of the same sample. ΔΔCT values were then obtained by calculating the difference between the ΔCT value of a given mRNA in CLM-citrate or CLM-succinate, and the ΔCt value of the same mRNA in CLM-glucose. Relative mRNA level values resulted from calculating $2^{-\Delta\Delta CT}$ values: values above 2.0 and below -0.5 show a higher and a lower mRNA level, respectively, in citrate or succinate supplementation compared to glucose supplementation.

Results and discussion

1. *P. aeruginosa* proteomic analysis reveals broad physiological changes upon carbon source supplementations

To ascertain the global effect of carbon sources on *P. aeruginosa* physiology, a quantitative proteomic study of the intracellular compartment was performed using cultures of *P. aeruginosa* PA14 grown in controlled liquid medium (CLM)-glucose, -glutamate, -succinate or -citrate. A total of 581 proteins were identified as differentially expressed in the 4 conditions, with a significant fold change (≥ 2) (Table S2). A principal component analysis (PCA) regrouping the proteomic data clearly revealed that the CLM-citrate condition is distinct from the other 3 conditions (Figure S1B). Among the 581 proteins, we found that 245, 130, 145 and 61 proteins were more abundant in CLM-citrate, CLM-glucose, CLM-glutamate, and CLM-succinate, respectively (Table S2). These quantitative proteomic data provided evidences that the carbon source supplementation affects the bacterial behavior.

We thus searched for biomarkers of each carbon source (Figure 1). A PCoA confirms that the CLM-citrate condition stands out from the 3 other conditions (Figure S1A). Among the 30 potential biomarkers involved in different biological functions, 7 proteins were clearly over-expressed in CLM-citrate (Figure 1 pink frame) while all other biomarkers were under-expressed in this condition. Then, 6 biomarkers were over-expressed in CLM-glucose (Figure 1 blue

frame), 11 in CLM-glutamate (Figure 1 purple frame) and 3 in CLM-succinate (Figure 1 orange frame). In the latter, PA14_68260 (dicarboxylate-binding protein) appears specific. Even if all these biomarkers are involved in metabolic pathways (energy, amino acid, transporters…), it is clear that several proteins are specific to a carbon source supplementation.

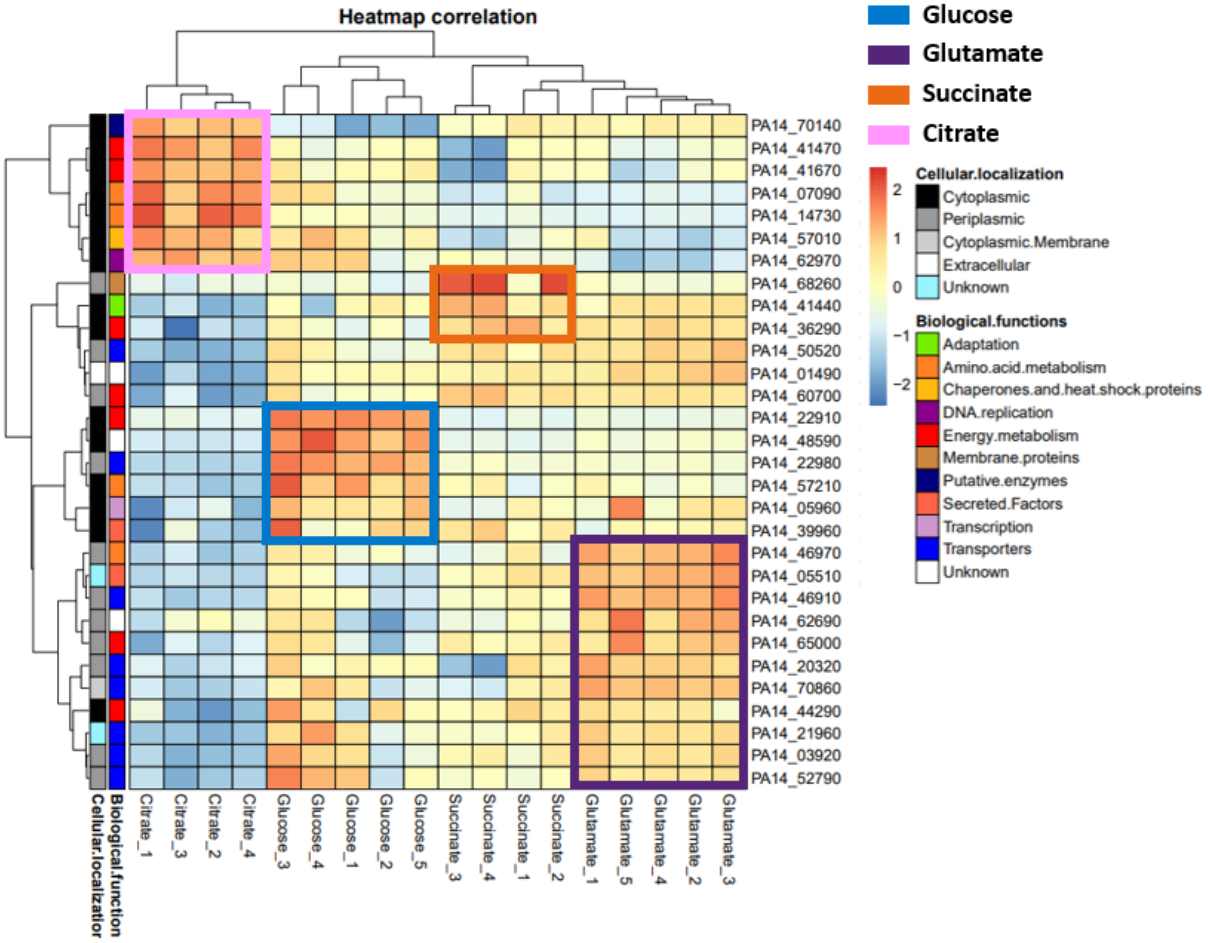

Figure 1. Heatmap hierarchical cluster representing the correlation in abundance variation of the 30 protein biomarkers.

By classifying the 548 proteins according to their function, we noticed that all conditions are represented in a large number of functions (Figure S7). However, there are some specific features since proteins involved in motility and attachment are more abundant only in the glucose condition, and those involved in antibiotic resistance are more abundant in the citrate condition. As expected, many proteins are hypothetical with unknown functions.

2. Citrate modulates virulence mechanisms in *P. aeruginosa*

P. aeruginosa possesses a large arsenal of virulence systems allowing them to colonize various hosts [31-32]. Some of them are involved in acute infection, while others operate during chronic infection. The activation of these different virulence systems depends on the environment in which the bacteria evolve, and therefore on the different carbon sources available [5].

Secreted factors

Proteins secreted by type 2, 3 and 6 secretion systems (T2SS, T3SS and T6SS respectively) were found differentially expressed. Among the virulence factors secreted by T2SS, the elastases LasB and LasA were accumulated when bacteria were grown in CLM-citrate (6 and 25-fold, respectively) (Table S2). By contrast, CbpD, a chitin-oxidizing virulence factor, was more abundant in CLM-succinate. As these virulence factors are secreted, a proteomic approach was performed to quantify them in the extracellular medium (Table S3). Unexpectedly, LasA and LasB were found less abundant in CLM-citrate compared to the other carbon sources. No differential expression was noticed for CbpD. In the extracellular medium, the virulence factor phospholipase C (PlcB), a hemolytic activity generating cell membrane destruction and tissue invasion [33], and the protease AprA were found also less abundant in CLM-citrate (Table S3). The effectors PcrV, PopB and SpcS (chaperone of ExoT) of T3SS were found more abundant in CLM-citrate with high fold changes (25, 9 and 426-fold, respectively) (Table S2). In the extracellular medium, PopB and the secreted toxin ExoU were also found more abundant in the condition CLM-citrate with high fold changes (143 and 11-fold, respectively) (Table S3). Only two proteins of T6SS, *i.e.* Tss1 (PA14_01020) and Hcp1 (PA14_01030), were observed to be less abundant in CLM-citrate while highly abundant in presence of the other carbon sources, especially in CLM-succinate (6 and 5-fold) (Table S2).

Pyocyanin is another major secreted virulence factor of *P. aeruginosa*. In presence of succinate, it has been suggested that *P. aeruginosa* produces less pyocyanin [34-35]. Indeed, the catabolite repression control (Crc) protein represses the production of pyocyanin by interacting with the mRNA of PhzM, which encodes a key enzyme in pyocyanin biosynthesis. Here, in agreement with this, PhzM was less abundant in CLM-succinate, while it was more abundant in CLM-citrate (Table S2). However, the pyocyanin assay did not confirmed a decrease of pyocyanin production in CLM-succinate compared to CLM-citrate (Figure 2). It is noteworthy that pyocyanin production is complex and tightly regulated. Moreover, it is only produced when PhzS and NADH are present because a transient physical interaction is required to activate pyocyanin production [36].

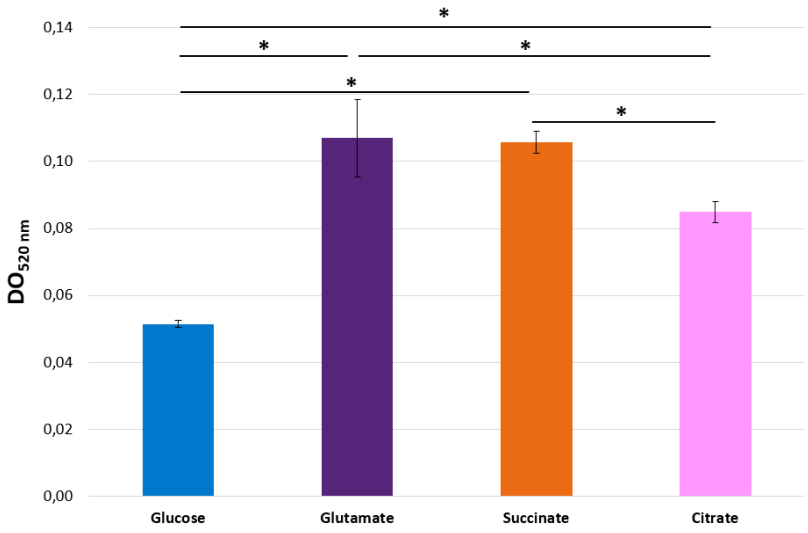

Figure 2. Pyocyanin production in *P. aeruginosa* PA14 grown in CLM supplemented with glucose, glutamate, succinate, or citrate.

In order to investigate the impact of carbon sources on bacterial global virulence expression, we exposed A549 pneumocytes to *P. aeruginosa* grown in the presence of the different carbon sources. After 6 hours of contact (time of infection), the amount of lactate dehydrogenase lactate dehydrogenase (LDH) released by disrupted A549 cells was quantified. We observed no impact

of the different supplementations of carbon sources in the ability of *P. aeruginosa* to destabilize A549 cells viability.

Altogether, these data suggest that *P. aeruginosa* would be more virulent in CLM-citrate and CLM-succinate. Nevertheless, our investigations suggest that none of these carbon source supplementations enhances the virulence of *P. aeruginosa* in host. One explanation could be that other virulence systems than those tested here are triggered to colonize hosts. Another hypothesis is that the medium is rich enough that *P. aeruginosa* do not have to be virulent to get the nutrients they need to grow [5]. Furthermore, we can also suggest that these proteins may be involved in another function than virulence.

Quorum-sensing

In *P. aeruginosa*, it is well known that virulence factors are regulated by *QS*, a communication system between bacteria. Three *QS* systems are reported in *P. aeruginosa* (Las, Rhl and Pqs systems). The Las and Rhl *N*-acyl-homoserine lactones (AHL) based-*QS* are composed by a synthase protein (LasI and RhlI, respectively) which is involved in the synthesis of AHLs signalling molecules and their cognate regulator (LasR and RhlR, respectively). The Pqs system involves the PqsABCD operon which is implicated in the formation of 4-hydroxy-2-heptylquinoline (HHQ), a precursor of *Pseudomonas* quinolone signal (PQS), and PqsH which allows the conversion of HHQ in PQS. The quantitative proteomic data revealed higher abundance of PqsB, PqsC, PqsD and PqsH in CLM-citrate (Table S2) suggesting enhanced production of PQS signaling molecules. To validate this, PQS production was quantified using HPLC-MS/MS. Accordingly, it was enhanced almost two times more in CLM-citrate as compared to the other carbon sources (Figure 3). In the literature, it was shown that a high concentration of PQS leads to extend the lag phase and to decrease the growth rate of *P. aeruginosa* under aerobic conditions [37]. According to this, we observed a delayed of growth of *P. aeruginosa* in the

CLM-citrate (Figure S8). All these results show that Pqs *QS* system is predominantly activated by citrate supplementation.

The Pqs *QS* system regulates the biosynthesis of pyocyanin. From proteomic data, we noticed 7 proteins implicated in the phenazine biosynthesis, a marker of PQS activity [38] and a virulence factor of *P. aeruginosa*. PhzE1, PhzF1, PhzH and PhzM were more abundant in CLM-citrate, PhzB2 and PhzG1 in CLM-glucose, and PhzD1 in CLM-succinate (Table S2).

We quantified by HPLC-MS/MS the small signalling molecules implicated in AHL based-*QS* mainly *N*-(3-oxododecanoyl)-L-homoserine lactone (3-oxo-C_{12}-HSL) produced by LasI and *N*-(butanoyl)-L-homoserine lactone (C_4-HSL) produced by RhlI (Figure 3). The 3-oxo-C_{12}-HSL was almost absent in all conditions except in CLM-glucose. This compound is produced at the beginning of the exponential phase, and interacts with LasR to regulate the expression of multiple virulence factors like exotoxin A (ToxA), LasA and LasB [39]. Then, when activated, LasR regulates positively RhlI/RhlR and PqsABCDH/PqsR, which are positively self-regulated by C_4-HSL and PQS, respectively. We observed that C_4-HSL was highly abundant in CLM-glucose and almost not in the other carbon sources (Figure 3).

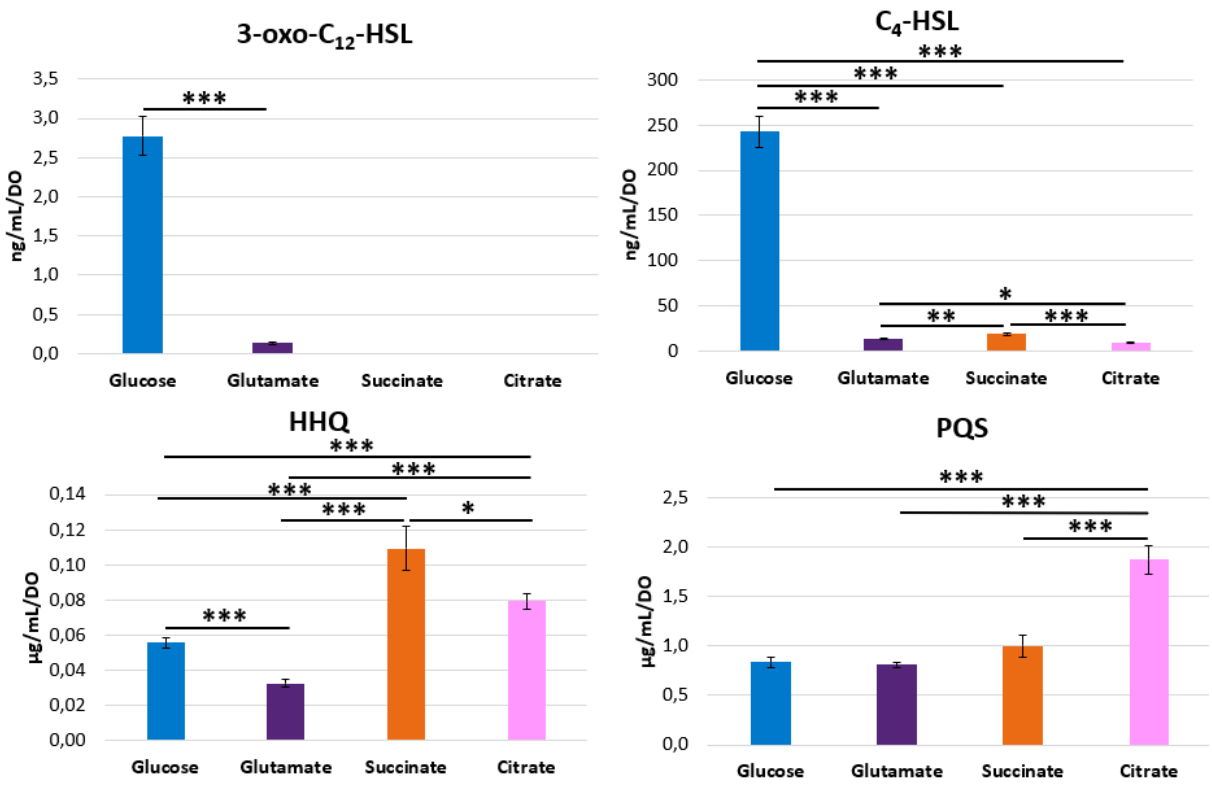

Figure 3. Quantification of *QS* molecules (3-oxo-C_{12}-HSL, C_4-HSL, HHS and PQS) by HPLC-MS/MS in the extracellular compartment of *P. aeruginosa* PA14 grown in CLM supplemented with glucose, glutamate, succinate, or citrate.

Iron uptake

In iron depletion conditions, *P. aeruginosa* uses different iron acquisition mechanisms for its survival. Several proteins known to be expressed in iron-rich condition (i.e. OprG [40]) were down-regulated in CLM-citrate. Otherwise, proteins known to be over-expressed in iron-limited condition (i.e. SdhA [41] or IcmP [42] were more abundant in CLM-citrate compared to other carbon sources supplementation (Table S2). These observations suggest that iron deficiency occurs in CLM-citrate. Indeed, four proteins (PchDEFG) involved in the synthesis of the pyochelin siderophore were recovered with high fold changes in CLM-citrate (18, 5, 68 and 63-fold, respectively) (Table S2). However, Cox et al. observed that ferric citrate uptake was not correlated with pyochelin synthesis and that the mechanism of ferric citrate uptake was not

induced by citrate [43]. They also noted that the bacterial mechanisms of iron uptake from ferric citrate were present in cells grown in a variety of media and were at their lowest level in cells grown in citrate.

Proteins implicated in the iron-sulfur (Fe-S) cluster biosynthesis (IscARSU and HscAB) were also more abundant in CLM-citrate (Table S2). This pathway is autoregulated by IscR, whose binding to [2Fe-2S] inhibits the transcription of this operon [44]. The up-regulation of these proteins suggested that CLM-citrate would be an iron limitation condition.

Another evidence of iron deficiency in CLM-citrate is the high concentration of PQS in the extracellular compartment (*cf.* section "*Quorum sensing*" and Figure 3). Indeed, PQS is a chelator of ferric iron (Fe^{3+}) and may facilitate the action of siderophores [37]. Due to the chelation of ferrous iron (Fe^{2+}) by citrate, we were not able to quantify iron acquisition by a chrome azurol sulphonate assay. The presence of such a complex may also restrict the availability of iron, though it can also be assumed that iron could be assimilated by *P. aeruginosa* in the form of this citrate/iron complex. Consequently, the concentration of free iron in the cell may be too high, which is toxic for the bacteria due to the Fenton reaction. *P. aeruginosa* may use bacterioferritins to scavenge iron and avoid Fenton reaction. Accordingly, BfrA and BfrB, two proteins involved in Fe^{2+} storage, were more abundant in CLM-citrate compared to the other carbon sources (11 and 7-fold, respectively) (Table S2).

3. Citrate alters motility and biofilm development in *P. aeruginosa*

Motility

Motility and chemotaxis of *P. aeruginosa* has been described as necessary for host colonization and virulence [45]. Bacterial motility is a complex process and the ability to move can be substantially impacted by the environmental conditions and thus the available carbon sources.

By proteomics, FleQ, the master regulator of flagellar biosynthesis (Table S2), and three flagellar components (FliD, FlgE, FlgK) (Table S3) were founded more abundant in CLM-citrate. Likewise some proteins belonging to the Che clusters I and II which modulate swimming motility [46] were altered according to the carbon source. CheB and CheZ of the Che cluster I were both more abundant in CLM-citrate, whereas CheR and CheV of the Che cluster II were more abundant in CLM-glucose and CLM-glutamate, respectively (Table S2).

Chemosensory systems have multiple functions as mediating chemotaxis, type IV pili-based motility or alternative cellular processes [45]. However, the function of the majority of chemoreceptors in *P. aeruginosa* is not yet established. Here, three probable methyl-accepting chemotaxis transducers (MCP) were detected. Thus, PA14_28050, a probable chemotaxis transducer described as a type IV pili methyl-accepting chemotaxis transducer in PFAM (PF13675) was more abundant in CLM-citrate. Both the uncharacterized PA14_39560 and the anoxic-responsive chemotaxis transducer Aer-2 (PA14_02220) were up-regulated in CLM-glutamate (Table S2).

Twitching motility in *P. aeruginosa* is controlled by a complex chemosensory pathway. Among proteins of this pathway, only ChpA, involved in biogenesis and chemosensing by type IV pili, was more abundant in CLM-succinate (Table S2).

P. aeruginosa motility was assessed in the 4 media (Figure 4). Noticeably, the three types of motility were reduced when *P. aeruginosa* PA14 was grown in CLM-citrate. To get further insights into this phenotype, atomic force microscopy (AFM) observations were performed. Planktonic PA14 grown in CLM-citrate showed usual rod-shaped bacteria with no flagella. However, numerous flagella fragments ranging from 0.5 µm to 5 µm were usually observed all around bacterial cells. While flagella fragments were also observed in planktonic bacteria grown in the other media, the ratio of flagella fragments over bacteria is far higher in CLM-citrate. This phenomenon may be due to a higher weakness of flagella when PA14 was grown

in CLM-citrate, which may explain the low swimming or swarming motilities of PA14 in this condition.

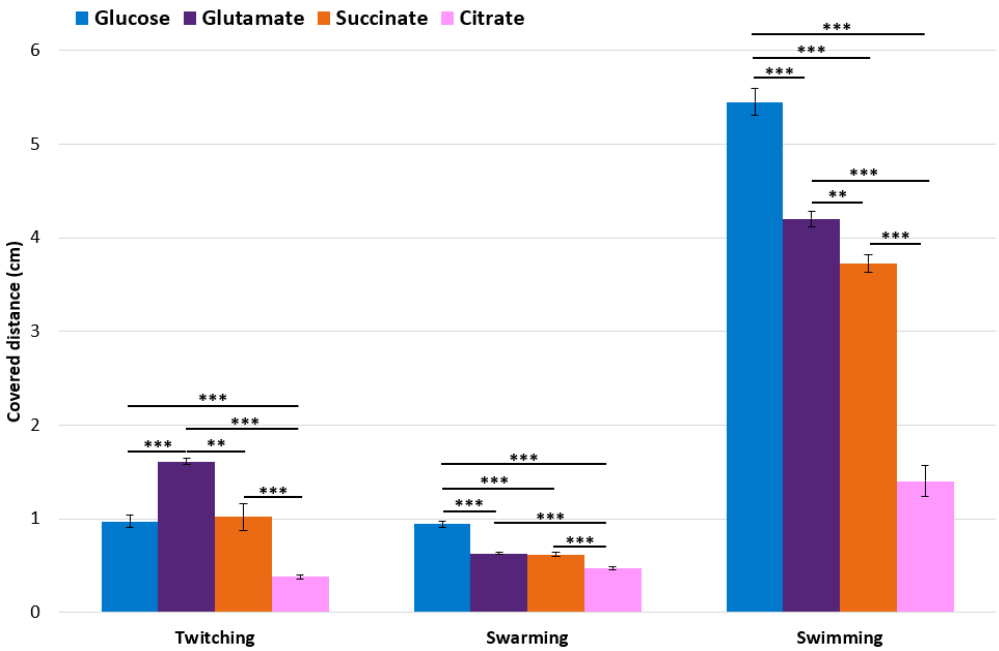

Figure 4. Distance covered with the different types of motility by *P. aeruginosa* PA14 grown in CLM supplemented with glucose, glutamate, succinate or citrate.

A carbon source supplementation seems to modulate the motility of *P. aeruginosa*. Proteomic and phenotypic results validated this hypothesis for a glucose, glutamate and succinate supplementations. Compared to citrate, a glucose, glutamate and succinate supplementations promotes all three types of motility. On the other hand, proteomic data showed that citrate supplementation seems to promote swimming motility while phenotypic assays point out that swimming motility is impaired. Actually, these results are consistent since AFM analysis revealed a weakness of the flagellum of *P. aeruginosa* grown in CLM-citrate, supporting the extensive production of flagellum proteins to replace them.

Biofilm formation

Biofilms are matrix-enclosed bacterial populations adherent to each other and/or to surfaces or interfaces [47]. This sessile lifestyle contributes to the resistance of bacteria against environmental stresses including antibiotic treatments [10]. Using both crystal violet (CV) assays and AFM observations, we investigated the ability of *P. aeruginosa* to form biofilm when grown with different carbon source supplementations. A strong biofilm formation was observed in CLM-glutamate, whereas a substitution by CLM-succinate slightly decreased it, and that by CLM-citrate and CLM-glucose led to a low biofilm formation (Figures 5A and 5B), suggesting the impact of carbon source in the biofilm development. In CLM-citrate, small sparse biofilm islands were observed (6 µm), as already described by Heydorn *et al.* [48]. Previously, Sauer *et al.* have shown that the genes *ccpR*, *nirS*, *ccoP2*, *nosZ*, *oprG* and *pa14_72260* were significantly increased in *P. aeruginosa* biofilm cells grown in presence of citrate [49]. Thus, it is not surprising to find the 6 corresponding proteins (CcpR, NirS, CcoP2, NosZ, OprG and PA14_72260) less abundant in CLM-citrate, as well as lectin A (LecA), an adhesion factor involved in biofilm development (Table S2).

Rhamnolipids are important components of *P. aeruginosa* biofilm [50]. They play multiple roles in biofilm development according to their concentration. In fact, a low concentration of rhamnolipids promotes biofilm formation [51] whereas a high concentration leads to biofilm dispersion [52-53]. By HPLC-MS/MS, we quantified 17 out of 20 rhamnolipids. They were obviously more abundant in CLM-glucose (Figure S9), suggesting a dispersal role for rhamnolipids in this condition. Moreover, no biofilm was observed by confocal laser scanning microscopy (CLSM) when cells were grown in CLM-glucose, supporting this hypothesis (Figures 5C and 5D).

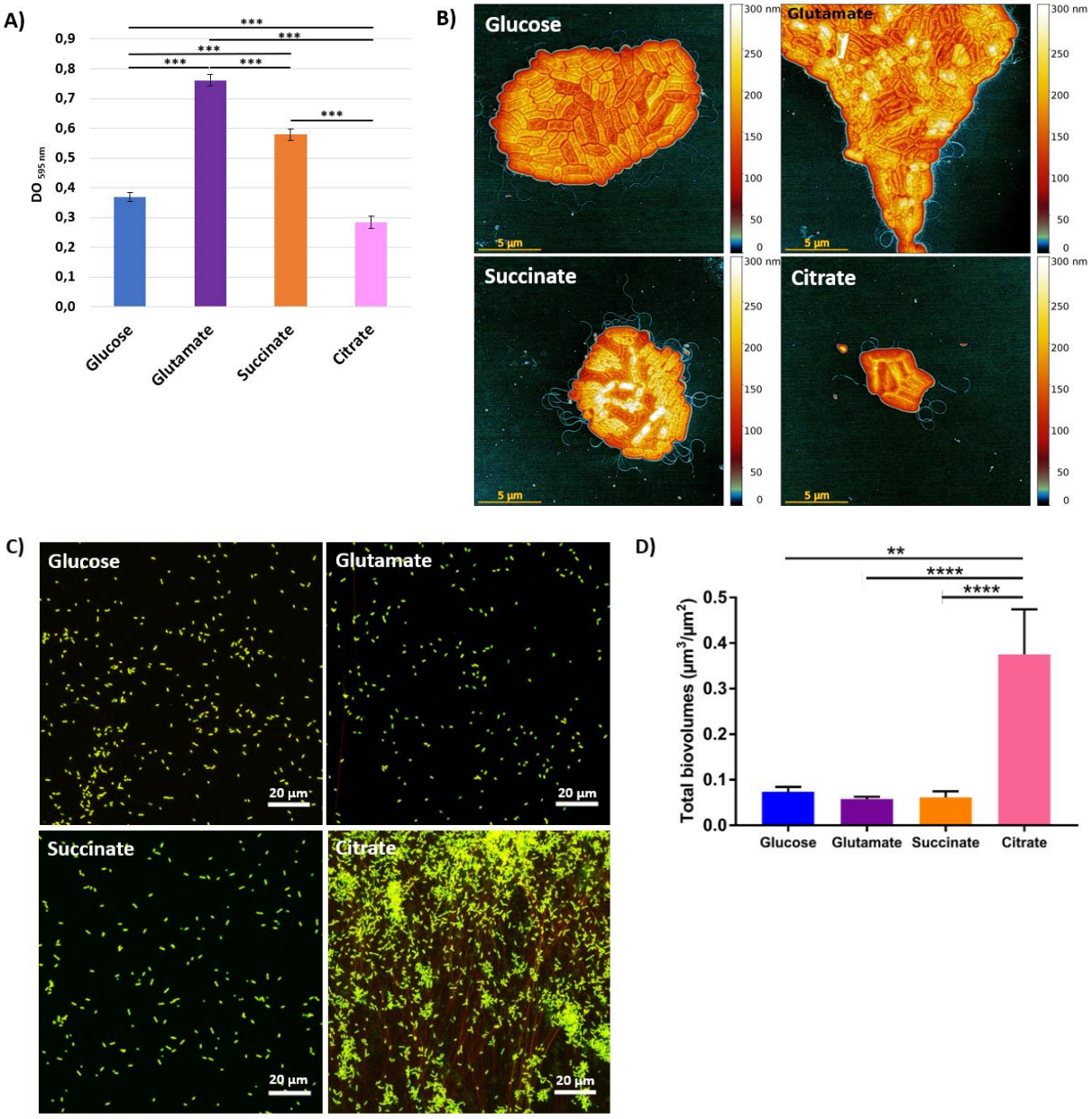

Figure 5. Biofilm investigations of *P. aeruginosa* PA14 grown in CLM supplemented with glucose, glutamate, succinate or citrate by A) crystal violet assay, B) AFM and C) CLSM. D) Total bio-volume ($\mu m^3/\mu m^2$) of 24-hours-old *P. aeruginosa* PA14 biofilms. Quantification of bio-volume was based on the confocal fluorescence images of Syto9 stained biofilms.

In addition, some mushroom structures and a large amount of extracellular DNA (eDNA) were surprisingly observed in CLM-citrate while no biofilm was seen in other conditions (Figures 5C and 5D). According to the literature, the stalk-forming subpopulation of the biofilm

produces eDNA via PQS, to which motile bacteria bind using type IV *pili*, initiating cap formation [50]. This is in accordance with our results in CLM-citrate where the concentration of PQS is clearly higher (Figure 3) and the type IV pilin structural subunit PilA is more abundant (Table S3) compared to the other carbon sources. In agreement with these observations, media supplemented with glucose, glutamate or succinate were not iron deficient, and this high concentration of iron in the medium suppressed *pqs* genes expression, DNA release and structural biofilm development [54].

Next, we investigated the expression of some genes involved in biofilm regulation, i.e. *cdrA*, *algU*, *amrZ*, *cmaX* and *dksA* (Figure S10). *cdrA* is positively regulated by c-di-GMP and promotes biofilm formation. It was over-expressed in CLM-succinate compared to CLM-glucose, whereas no significant difference was observed in CLM-citrate. AlgU enhances biofilm development at least via overexpression of genes encoding the exopolysaccharide alginate, and manages the expression of *amrZ*, *cmaX* and *dksA*. It was significantly under-expressed in CLM-citrate and CLM-succinate compared to CLM-glucose. However, AlgU targets, except *cmaX*, were significantly overexpressed in CLM-citrate and CLM-succinate compared to CLM-glucose, suggesting that AlgU was active in these conditions.

CV assay, AFM observations and proteomic analysis suggested that glutamate supplementation promotes biofilm development while citrate supplementation reduced it. CLSM and qRT-PCR suggested the opposite. This disagreement could be explained by the different surface used depending on the techniques, but they still allowed us to compare the results according to the different carbon source supplementations within the same assay. Moreover, in contrast to previous studies, here we used more than one carbon source and at non-limiting concentrations. Finally, we can assume that the effect of the carbon sources also depends on other environmental parameters such as the timing of their addition or whether the biofilm is made under static or dynamic conditions.

4. Citrate increases the resistance of *P. aeruginosa* to several antibiotics

Antibiotic resistance

P. aeruginosa is highly resistant to a wide range of antibiotics, including aminoglycosides, quinolone and β-lactams, making its infections very difficult to treat, especially in biofilm consortium [16]. This remarkable capacity for antibiotic resistance may be enhanced or impaired by the carbon sources available during growth [55].

Proteomic data showed that MexA and OprM were more abundant in CLM-citrate as compared to other carbon sources supplementation. The abundance of MexR, the regulator of MexAB-OprM efflux pump, was also increased in CLM-citrate (Table S2). The MexAB-OprM efflux pump is one of the mechanisms of intrinsic resistance of *P. aeruginosa* to β-lactams. These antibiotics are inhibitors of the peptidoglycan synthesis by acting on transpeptidases and carboxypeptidases, and penicillin binding proteins [56]. To determine whether carbon source supplementations impact *P. aeruginosa* antibiotics susceptibility, we determined minimum inhibitory concentration (MIC) values for different antibiotics. MICs show an increase in resistance to ticarcillin and ceftazidime in CLM-citrate and CLM-succinate, and to imipenem in CLM-succinate, compared to CLM-glucose, our reference medium (Table 1). MexAB-OprM is also the only system that is expressed constitutively in cells grown in standard laboratory media. This suggests that the export of antimicrobial agents is not the primary function of this pump. Indeed, it was reported that MexAB-OprM is overexpressed under iron limitation conditions, suggesting that this pump plays an essential role in the survival of *P. aeruginosa* under iron limitation conditions [57-59]. Since citrate can function as an iron chelator, the over-expression of MexAB-OprM may be also explain by iron depletion (*cf*. above *Iron uptake*).

Table 1. MICs of *P. aeruginosa* PA14 grown in CLM supplemented with glucose, glutamate, succinate or citrate. In red are indicated >2-fold MICs values as compared to MICs values determined in glucose supplementation.

Antibiotics family	Antibiotics (µg/mL)	Glucose	Glutamate	Succinate	Citrate
Polymyxins	Colistin	0.5	1	**16**	**512**
β-lactamines (Penicillin)	Ticarcillin	8	16	**32**	**32**
β-lactamines (Cephalosporins)	Ceftazidime	0.25	0.5	**1**	**2**
β-lactamines (Carbapenems)	Imipenem	1	2	**4**	1
Quinolones	Ciprofloxacin	0.0625	0.031	0.0625	0.03125
Aminoglycosides	Gentamicin	0.5	**2**	**2**	**4**
Aminoglycosides	Tobramycin	0.5	1	**2**	**2**
Cyclins	Tetracycline	2	4	4	2

By quantitative proteomic, we pointed out higher abundance levels of proteins involved in *P. aeruginosa* resistance to colistin, a polycationic antimicrobial peptide belonging to the polymyxin class of antibiotics, in CLM-citrate. This includes different regulators of two-component systems and some of their protein targets (PhoP, OprH, ArnA, ArnB and PmrA) (Table S2). PhoP belongs to the two-component system PhoP/PhoQ [60-61] which is known to be induced by Mg^{2+} starvation [62]. It positively regulates the production of the porin OprH, a protein implicated in the outer membrane stability and reducing the effect of colistin against the bacteria. A second mechanism involved in colistin resistance concerns the *arn* operon. The products of these genes are involved in the production of 4-amino-4-deoxy-L-arabinose, and to anchor it to the lipid A of the lipopolysaccharide (LPS) [63], thus increasing the bacterial surface positive charge. PmrA promotes the synthesis of N4-aminoarabinose, modifying the phospholipid charge and therefore

the global net charge of the membrane. We tried to measure the membrane surface charge of *P. aeruginosa* grown in the different carbon sources using the Zeta potential [64]. Unfortunately, no charge difference was observed suggesting that these carbon sources did not significantly modify the membrane charge.

Thus, proteomic results suggest that, in CLM-citrate, *P. aeruginosa* would be more resistant to colistin. This was validated by MIC experiments since the resistance of PA14 to colistin was clearly higher in CLM-citrate than in media supplemented with other carbon sources (Table 1). Furthermore, our results showed that PA14 was also more resistant to tobramycin and gentamicin, two aminoglycosides targeting the 30S ribosomal unit, leading to produce altered proteins [65].

Bacterial membrane

The bacterial membrane plays an important role in antibiotic resistance (in particular in cell penetration) [66-67] and it has been shown that the nature of the carbon source can modify the membrane properties [1, 68].

To evaluate the influence of the carbon source supplementations on the membrane fluidity, fluorescence anisotropy (FAn) measurements were then performed. FAn value of *P. aeruginosa* grown in CLM-citrate was significantly higher than FAn value of *P. aeruginosa* supplemented with other carbon sources (Figure 6). These data suggest that citrate induces membranes stiffness for this strain. Interestingly, both OprF and OprH were observed more abundant in citrate (Table S2). OprF is the major porin in *P. aeruginosa* and plays a structural role since it allows the membrane to be anchored to the peptidoglycan increasing the envelope integrity [62]. OprH acts as a substitute of Mg^{2+}, and it cross-links LPS and thus tightens the outer membrane during divalent cation deficiency [65].

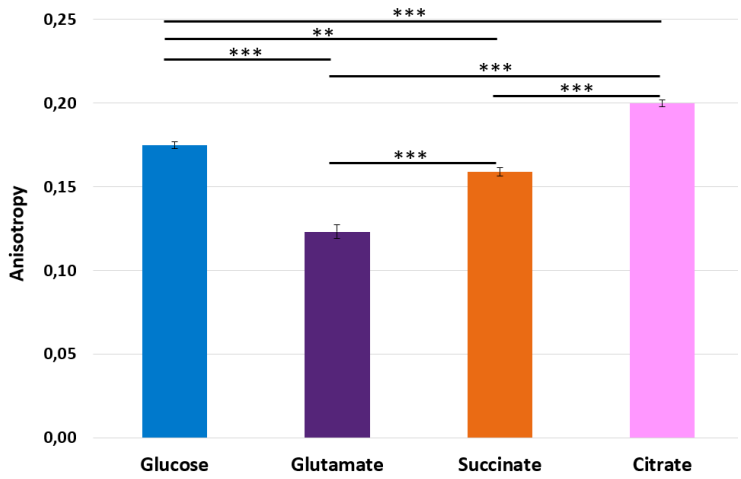

Figure 6. Membrane fluidity of *P. aeruginosa* PA14 grown in CLM supplemented with glucose, glutamate, succinate or citrate.

Noticeably, the extracytoplasmic function sigma factor SigX was shown to control membrane fluidity homeostasis [69-72] probably by regulating the expression of de novo fatty acids biosynthesis [73-74]. A sigX mutant was shown to display an increased membrane stiffness [69], while a strain overproducing SigX possessed a more fluid membrane [73]. In addition, Fléchard *et al.* demonstrated that SigX is indirectly involved in carbon catabolite repression regulation (via Crc and CrcZ), probably partly because of its enhanced stiffness and consequently loss of integrity and functionality [69]. Accordingly, *sigX* was up-regulated in CLM-succinate and down-regulated in CLM-citrate compared to CLM-glucose (Figure S10). This result is in agreement with a loss of the membrane fluidity in presence of citrate.

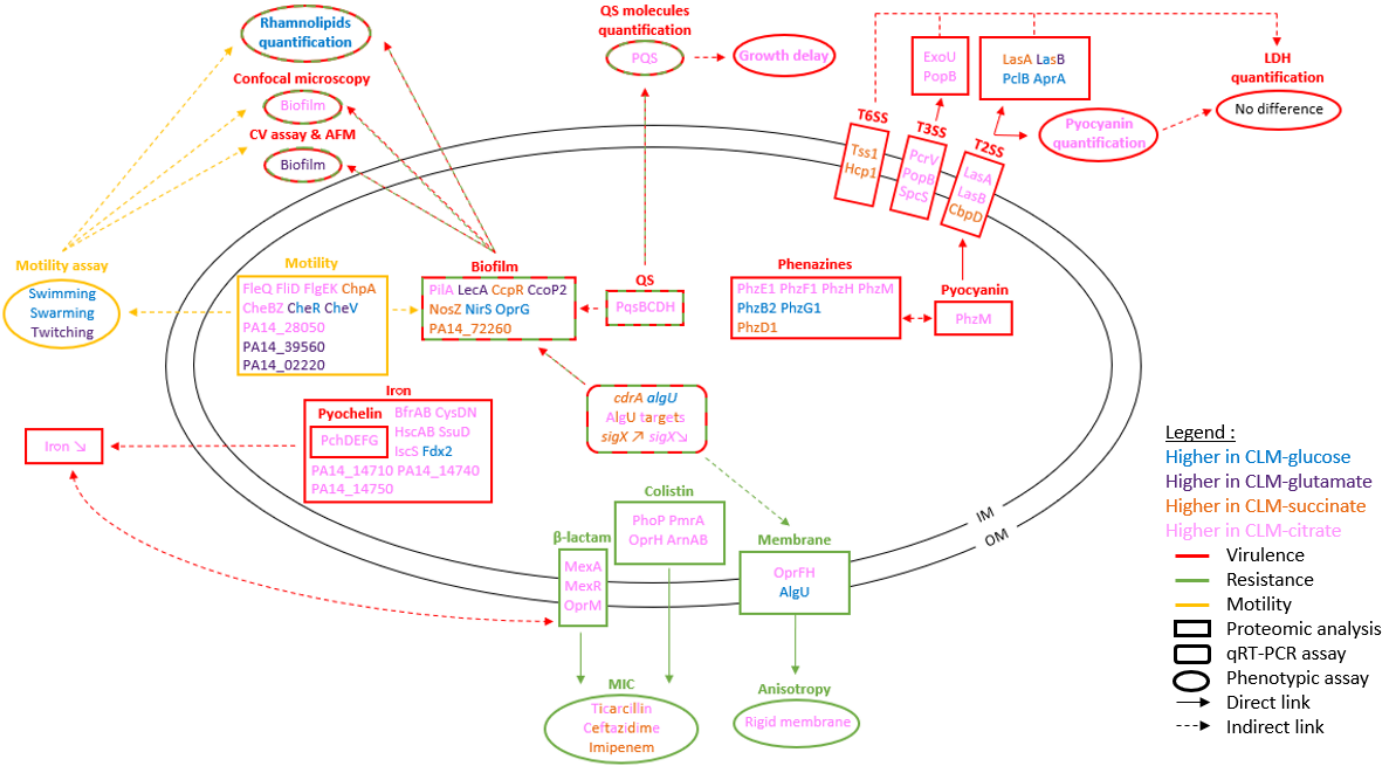

Figure 7. Overview of the different biological processes impacted by the different culture media supplemented with a carbon source (glucose, glutamate, succinate, or citrate) on *P. aeruginosa* strain PA14. Proteins, genes and phenotypic assays are indicated according to the condition, in which they are the most expressed. For sigX and iron, for which the arrows indicate an increase (↗) or a decrease (↘) in expression. AFM: atomic force microscopy; CLM: controlled liquid medium; CV: crystal violet; LDH: lactate dehydrogenase; MIC: minimum inhibitory concentration; IM: inner membrane; OM: outer membrane; PQS: *Pseudomonas* quinolone signal; QS: *quorum sensing*; T2SS: type 2 secretion system; T3SS: type 3 secretion system; T6SS: type 6 secretion system.

Conclusion

The current study shows that supplementation with carbon sources (*i.e.* glucose, glutamate, succinate or citrate) affects the physiology of *P. aeruginosa* PA14 summarized in figure 7 (Figure 7). In particular, citrate supplementation seems to have an important impact on many bacterial processes. Indeed, in *P. aeruginosa*, citrate supplementation limits its motility, impacts its biofilm development, and clearly increases its resistance to several antibiotics through the activation of protein networks known to be involved in antibiotic resistance and bacterial membrane modification. However, the impact of carbon source supplementations on virulence is more nuanced. Thus, supplementation with carbon sources promotes or alters the activation or repression of specific metabolic pathways in *P. aeruginosa*, highlighting the importance of the environment in which the bacterium evolves on its behavior.

In order to survive, *P. aeruginosa* must extract nutrients available in its habitat, while competing with other bacteria to be the first to exploit these resources. Bacterial species that process nutrients more efficiently might outgrow others [5]. Consequently, *P. aeruginosa* adapts its metabolism in order to survive, for example by secreting virulence factors to break down alternative nutrients available in its environment or to eliminate bacteria or cells living in the same ecological niche [75], or by switching to biofilm mode while waiting for a more suitable environment [49]. In this way, a better understanding of bacterial metabolism according to the nutrients available in its environment, using complementary experiments as proteomics and phenotypic assays, would lead to a better understanding of bacterial pathogenesis and thus to the identification of new strategies complementary or alternative to antibiotics to efficaciously combat these bacterial agents.

Supporting Information

The following files are available free of charge.

Supplementary Data S1: Extraction of RNA and analyses by qRT-PCR

Figure S1: A) Principal coordinate analysis (PCoA) comparing the level of variance among biological and technical replicates in the 4 growth conditions for the 30 potential biomarkers obtained after ANOVA one way. B) Principal component analysis (PCA) comparing the level of variance among biological and technical of *P. aeruginosa* PA14 grown in culture media supplemented with a carbon source (glucose, glutamate, succinate, or citrate).

Figure S2: EIC, MS and MS/MS spectra of A) C_4-HSL, B) 3-oxo-C_{12}-HSL, C) HHQ, and D) PQS. The full circles in the MS2 spectrum show the expected characteristic fragment ions and the dotted circles show the secondary fragment ions.

Figure S3: Calibration curves of A) standard molecules (C_4-HSL, 3-oxo-C_{12}-HSL, C_7-HSL, HHQ-D4 and PQS-D4) and B) zoom of HHQ-D4 and PQS-D4 (corresponding to the red square on A)). The area of EIC-peaks is linear on a wide range of mass (up to 3,000 pg) for the 3 AHLs. The linearity for HHQ-D4 and PQS-D4 is more restricted and is applied on a mass range below 500 pg.

Figure S4: Calibration curves established from EIC-peak areas of variable quantities of C_4-HSL or 3-oxo-C_{12}-HSL injected with a fixed quantity of C_7-HSL (250 pg).

Figure S5: Examples of EIC-peaks of rhamnolipids extracted from MS data. Examples are given for the major rhamnolipids: *m/z* 503.32 (R-C10-C10 / R-C8-C12/ R-C12-C8), *m/z* 531.35 (R-C10-C12 / R-C12-C10), *m/z* 649.38 (R-R-C10-C10 / R-R-C8-C12/ R-R-C12-C8) and *m/z* 677.41 (R-R-C10-C12 / R-R-C12-C10).

Figure S6: Calibration curve carried out from a commercial rhamnolipid mixture. The EIC areas were measured for all detected rhamnolipids from various amounts (2.5, 5, 10, 15, 20, 25, 30, 40, 50, 75, 100 et 150 ng) of the commercial solution. The proportions of each rhamnolipid is

determined by calculating the ratio of the individual area of each rhamnolipid to the sum of the areas of all rhamnolipids. These values are then reported in ng based on the total amount of the commercial mixture.

Figure S7: Functional classification of proteins found overexpressed in the intracellular quantitative proteomic analysis of *P. aeruginosa* PA14 grown in culture media supplemented with a carbon source (glucose, glutamate, succinate, or citrate).

Figure S8: Growth curves of *P. aeruginosa* PA14 grown in culture media supplemented with a carbon source (glucose, glutamate, succinate or citrate).

Figure S9: Rhamnolipids quantification of *P. aeruginosa* PA14 grown in culture media supplemented with a carbon source (glucose, glutamate, succinate or citrate).

Figure S10: Comparison of gene expression by qRT-PCR between *P. aeruginosa* PA14 grown in medium supplemented with glucose and media supplemented with succinate or citrate.

Table S1: List of genes tracked by qRT-PCR with their primers.

Table S2: List of the intracellular proteins differentially expressed in *P. aeruginosa* PA14 grown in culture media supplemented with a carbon source (glucose, glutamate, succinate, or citrate).

Table S3: List of the extracellular proteins differentially expressed in *P. aeruginosa* PA14 grown in culture media supplemented with a carbon source (glucose, glutamate, succinate, or citrate).

Table S4: List of the 30 potential biomarkers of *P. aeruginosa* PA14 grown in culture media supplemented with a carbon source (glucose, glutamate, succinate, or citrate).

Corresponding author

*Dr Julie Hardouin, Laboratoire Polymères, Biopolymères, Surfaces, UMR CNRS 6270, Université de Rouen, Bâtiment CURIB, 76821 Mont-Saint-Aignan cedex, France.

Tel: +33 (0)2 35 14 67 09

E-mail: julie.hardouin@univ-rouen.fr

Author Contributions

Conceptualization, S.S., C.G. and J.H.; methodology, S.S., C.G., A.T., L.C., H.L., S.A., E.B., O.L. and J.H.; formal analysis, S.S., C.G. and A.B.A.; investigation, S.S., C.G. and J.H.; writing-original draft, S.S., C.G. and J.H.; writing-review and editing, S.S., C.G., A.T., L.C., H.L., S.A., A.B.A., O.L., S.C., T.J. and J.H.; visualization, S.S.; supervision, J.H.; funding acquisition, J.H.; resources, A.T., L.C., H.L., S.A., E.B., O.L., S.C., and J.H. and S.C.; All authors have read and agreed to the published version of the manuscript.

Funding sources

S.S. is a recipient of doctoral fellowship from the Region Normandie (France). Work was co-supported by the European Union and Region Normandie. Europe gets involved in Normandie with European Regional Development Fund (ERDF).

Conflicts of Interest

The authors declare no conflict of interest.

Acknowledgments

We thank Delphine Vergoz from CNRS Polymers, Biopolymers, Surface Laboratory (Mont-Saint-Aignan, France) and Lea Duval (internship student from University of Rouen Normandy, France) for their assistance in conducting, processing, and analyzing some of the assays performed for this study. We also thank the laboratory of Pr Eric Déziel (Institut National de la Recherche Scientifique, Institut Armand Frappier, Canada) for providing us with HHQ-D4 and PQS-D4 necessary for the quantification of HHQ and PQS by mass spectrometry.

CLSM images were obtained on PRIMACEN (https://primacen.crihan.fr) (Cell Imaging Platform of Normandy, IRIB, Faculty of Sciences, University of Rouen, Mont-Saint-Aignan, France).

Abbreviations

ACN : acetonitrile ; AFM : atomic force microscopy ; AHL : *N*-acyl-homoserine lactone ; ANOVA : one-may analysis of variance ; C_4-HSL : *N*-butanoyl-homoserine lactone; C_7-HSL : *N*-heptanoyl-L-homoserine lactone ; C7BzO : 3-(4-heptyl)phenyl-3-hydroxypropyl)dimethylammoniopropanesulfonate ; CHAPS : 3-[(3-cholamidopropyl)dimethylammonio]-1-propanesulfonate hydrate ; CLM : controlled liquid medium ; CLM-glucose : CLM supplemented with glucose ; CLM-glutamate : CLM supplemented with glutamate ; CLM-succinate : CLM supplemented with succinate ; CLM-citrate : CLM supplemented with citrate ; CLSM : confocal laser scanning microscopy ; Crc : catabolic repression control ; CV : crystal violet ; DPH : 1,6-diphenyl-1,3,5-hexatriene ; DTT : dithiothreitol ; eDNA : extracellular DNA ; EIC : extracted-ion chromatogram ; FA : formic acid ; FAn : fluorescence anisotropy ; HHQ : 4-hydroxy-2-heptylquinoline ; HHQ-D4 : deuterated HHQ ; HPLC-MS/MS : high performance liquid chromatography coupled with mass spectrometry ; IM : inner membrane ; LC-MS/MS : liquid chro-

matography coupled with mass spectrometry ; LDH : lactate dehydrogenase ; LPS : lipopolysaccharide ; MCP : methyl-accepting chemotaxis transducers ; MHB : Mueller Hinton Broth ; MIC : minimum inhibitory concentration ; OM : outer membrane ; PBS : phosphate buffered saline ; PCA : principal component analysis ; PCoA : principal coordinate analysis ; PQS : *Pseudomonas* quinolone signal ; PQS-D4 : deuterated PQS ; *QS* : *quorum sensing* ; SDS : sodium dodecyl sulfate ; TCA : trichloroacetic acid ; TBP : tri-N-butylphosphine ; T2SS : type 2 secretion system ; T3SS : type 3 secretion system ; T6SS : type 6 secretion system ; 3-oxo-C_{12}-HSL : *N*-(3-oxododecanoyl)-L-homoserine lactone

References

1. Ene, I. E.; Adya, A. K.; Wehmeier, S.; Brand, A. C.; MacCallum, D. M.; Gow, N. A. R.; Brown, A. J. P., Host carbon sources modulate cell wall architecture, drug resistance and virulence in a fungal pathogen. *Cellular Microbiology* **2012,** *14* (9), 1319-1335.
2. Görner, W.; Durchschlag, E.; Brown, E. L.; Ammerer, G.; Ruis, H.; Schüller, C., Acute glucose starvation activates the nuclear localization signal of a stress-specific yeast transcription factor. *The EMBO Journal* **2002,** *21* (1&2), 134-144.
3. Rojo, F., Carbon catabolite repression in *Pseudomonas*: optimizing metabolic versatility and interactions with the environment. *FEMS Microbiology Reviews* **2010,** *34*, 658-684.
4. Sánchez, S.; Chávez, A.; Forero, A.; Garciá-Huante, Y.; Romero, A.; Sánchez, M.; Rocha, D.; Sánchez, B.; Avalos, M.; Guzmán-Trampe, S.; Rodríguez-Sanoja, R.; Langley, E.; Ruiz, B., Carbon source regulation of antibiotic production. *The Journal of Antibiotics* **2010,** *63*, 442-459.
5. Rohmer, L.; Hocquet, D.; Miller, S. I., Are pathogenic bacteria just looking for food? Metabolism and microbial pathogenesis. *Trends in Microbiology* **2011,** *19* (7), 341-348.
6. Perinbam, K.; Chacko, J. V.; Kannan, A.; Digman, M. A.; Siryaporn, A., A shift in central metabolism accompanies virulence activation in *Pseudomonas aeruginosa*. *mBio* **2020,** *11*, e02730-18.
7. Eisenreich, W.; Dandekar, T.; Heesemann, J.; Goebel, W., Carbon metabolism of intracellular bacterial pathogens and possible links to virulence. *Nature Reviews Microbiology* **2010,** *8*, 401-412.
8. Lorenz, M. C.; Fink, G. R., The glyoxylate cycle is required for fungal virulence. *Letters to Nature* **2001,** *412*, 83-86.
9. Bester, E.; Kroukamp, O.; Hausner, M.; Edwards, E. A.; Wolfaardt, G. M., Biofilm form and function: carbon availability affects biofilm architecture, metabolic activity and planktonic cell yield. *Journal of Applied Microbiology* **2010,** *110*, 387-398.
10. Rasamiravaka, T.; Labtani, Q.; Duez, P.; El Jaziri, M., The formation of biofilms by *Pseudomonas aeruginosa*: a review of the natural and synthetic compounds interfering with control mechanisms. *BioMed Research International* **2014,** *2015*, 759348.

11. O'Toole, G. A.; Kolter, R., Initiation of biofilm formation in *Pseudomonas fluorescens* WCS365 proceeds via multiple, convergent signalling pathways: a genetic analysis. *Molecular Microbiology* **1998,** *28* (3), 449-461.
12. Khan, F.; Thuy Nguyen Pham, D.; Folarin Oloketuyi, S.; Kim, Y.-M., Regulation and controlling the motility properties of *Pseudomonas aeruginosa*. *Applied Microbiology and Biotechnology* **2020,** *104*, 33-49.
13. Shrout, J. D.; Chopp, D. L.; Just, C. L.; Hentzer, M.; Givskov, M.; Parsek, M., The impact of *quorum sensing* and swarming motility on *Pseudomonas aeruginosa* biofilm formation is nutritionally conditional. *Molecular Microbiology* **2006,** *62* (5), 1264-1277.
14. Gaviard, C.; Broutin, I.; Cosette, P.; Dé, E.; Jouenne, T.; Hardouin, J., Lysine succinylation and acetylation in *Pseudomonas aeruginosa*. *Journal of Proteome Research* **2018,** (17), 2449-2459.
15. World Health Organization WHO publishes list of bacteria for which new antibiotics are urgently needed. https://www.who.int/news-room/detail/27-02-2017-who-publishes-list-of-bacteria-for-which-new-antibiotics-are-urgently-needed (accessed 17 April).
16. Pang, Z.; Raudonis, R.; Glick, B. R.; Lin, T.-J.; Cheng, Z., Antibiotic resistance in *Pseudomonas aeruginosa*: mechanisms and alternative therapeutic strategies. *Biotechnology Advances* **2019,** *37*, 177-192.
17. Azam, M. W.; Khan, A. U., Updates on the pathogenicity status of *Pseudomonas aeruginosa*. *Drug Discovery Today* **2019,** *24* (1), 350-359.
18. Sloss, J. M.; Cumberland, N.; Milner, S. M., Acetic acid used for the elimination of *Pseudomonas aeruginosa* from burn and soft tissue wounds. *Journal of the Royal Army Medical Corps* **1993,** *139*, 49-51.
19. Al-Ibran, E.; Khan, M., Efficacy of topical application of 1% acetic acid in eradicating pseudomonal infections in burn wounds. *Journal of the Dow University of Health Sciences* **2010,** *4*, 90-93.
20. Juma, I. M.; Yass, H. a. S.; Al-Jaberi, F. H., A comparison between the effect of acetic acid and salicyclic acid in different concentrations on *Pseudomonas aeruginosa* isolated from burn wound infections. *Journal of Techniques* **2007,** *20* (1), 23-78.
21. Nagoba, B.; Wadher, B.; Kulkarni, P.; Kolhe, S., Acetic acid treatment of pseudomonal wound infections. *European Journal of General Medicine* **2008,** *5* (2), 104-106.
22. Nagoba, B. S.; Deshmukh, S. R.; Wadher, B. J.; Mahabaleshwar, L.; Gandhi, R. C.; Kulkarni, P. B.; Mane, V. A.; Deshmukh, J. S., Treatment of superficial pseudomonal infections with citric acid: an effective and economical approach. *Journal of Hospital Infection* **1998,** *40* (2), 155-157.
23. Nagoba, B. S.; Gandhi, R. C.; Wadher, B. J.; Gandhi, S. P.; Deshmukh, S. R., Citric acid treatment of severe electric burns complicated by antibiotic resistant *Pseudomonas aeruginosa*. *Burns* **1998,** *24*, 481-483.
24. Gaviard, C.; Cosette, P.; Jouenne, T.; Hardouin, J., LasB and CbpD virulence factors of *Pseudomonas aeruginosa* carry multiple post-translational modifications on their lysine residues. *Journal of Proteome Research* **2019,** (18), 923-933.
25. Winsor, G. L.; Griffiths, E. J.; Lo, R.; Dhillon, B. K.; Shay, J. A.; Brinkman, F. S. L., Enhanced annotations and features for comparing thousands of *Pseudomonas* genomes in the Pseudomonas genome database. *Nucleic Acids Research* **2016,** *44* (Database issue).
26. Park, A. J.; Murphy, K.; Krieger, J. R.; Brewer, D.; Taylor, P.; Habash, M.; Khursigara, C. M., A temporal examination of the planktonic and biofilm proteome of whole cell *Pseudomonas aeruginosa* PAO1 using quantitative mass spectrometry. *Molecular and Cellular Proteomics* **2014,** *13.4*.

27. R Core Team *R: A Language and Environment for Statistical Computing*, 4.1; R Foundation for Statistical Computing, Vienna, Austria.: 2020.
28. Lakowicz, J. R., Fluoresecnce spectroscopy. In *Principles of fluoresecnce spectroscopy*, Springer, Ed. Springer: 2006; pp 353-382.
29. Le, H.; Arnoult, C.; Dé, E.; Schapman, D.; Galas, L.; Le Cerf, D.; Karakasyan, C., Antibody-conjugated nanocarriers for targeted antibiotic delivery: application in the treatment of bacterial biofilms. *Biomacromolecules* **2021,** *22* (4), 1639-1653.
30. Bouffartigues, E.; Gicquel, G.; Bazire, A.; Bains, M.; Maillot, O.; Vieillard, J.; Feuilloley, M. G. J.; Orange, N.; Hancock, R. E. W.; Dufour, A.; Chevalier, S., Transcription of the *oprF* gene of *Pseudomonas aeruginosa* is dependent mainly on the SigX sigma factor and is sucrose induced. *Journal of Bacteriology* **2012,** *194* (16), 4301-4311.
31. Kipnis, E.; Sawa, T.; Wiener-Kronish, J., Targeting mechanisms of *Pseudomonas aeruginosa* pathogenesis. *Médecine et maladies infectieuses* **2006,** *36*, 78-91.
32. Morin, C. D.; Déziel, E.; Gauthier, J.; Levesque, R. C.; Lau, G. W., An organ system-based synopsis of *Pseudomonas aeruginosa* virulence. *Virulence* **2021,** *12* (1), 1469-1507.
33. Terada, L. S.; Johansen, K. A.; Nowbar, S.; Vasil, A. I.; Vasil, M. L., *Pseudomonas aeruginosa* hemolytic phospholipase C suppresses neutrophil respiratory burst activity. *Infection and Immunity* **1999,** *67* (5), 2371-2376.
34. Huang, J.; Sonnleitner, E.; Ren, B.; Xu, Y.; Haas, D., Catabolite repression of pyocyanin biosynthesis at an intersection of primary and secondary metabolism in *Pseudomonas aeruginosa*. *Applied and Environmental Microbiology* **2012,** *78*, 5016-5020.
35. Lau, G. W.; Hassett, D. J.; Ran, H.; Kong, F., The role of pyocyanin in *Pseudomonas aeruginosa* infection. *Trends in Molecular Medicine* **2004,** *10* (12), 599-606.
36. Parsons, J. F.; Greenhagen, B. T.; Shi, K.; Calabrese, K.; Robinson, H.; Ladner, J. E., Structural and functional analysis of the pyocyanin biosythetic protein PhzM from *Pseudomonas aeruginosa*. *Biochemistry* **2007,** *46* (7), 1821-1828.
37. Lin, J.; Cheng, J.; Wang, Y.; Shen, X., The *Pseduomonas* quinolone signal (PQS): not just for *quorum sensing* anymore. *Frontiers in Cellular and Infection Microbiology* **2018,** *8*, 230.
38. Mould, D. L.; Botelho, N. J.; Hogan, D. A., Intraspecies signaling between common variants of *Pseudomonas aeruginosa* increases production of *quorum sensing*-controlled virulence factors. *mBio* **2020,** *11* (4), e01865-20.
39. Strateva, T.; Mitov, I., Contribution of an arsenal of virulence factors to pathogenesis of *Pseudomonas aeruginosa* infections. *Annals of Microbiology* **2011,** *61*, 717-732.
40. McPhee, J. B.; Tamber, S.; Bains, M.; Maier, E.; Gellatly, S.; Lo, A.; Benz, R.; Hancock, R. E. W., The major outer membrane protein OprG of *Pseudomonas aeruginosa* contributes to cytotoxicity and forms an anaerobically regulated, cation-selective channel. *FEMS Microbiology Letters* **2009,** *296*, 241-247.
41. Wakeman, C. A.; Moore, J. L.; Noto, M. J.; Zhang, Y.; Singleton, M. D.; Prentice, B. M.; Gilston, B. A.; Doster, R. S.; Gaddy, J. A.; Chazin, W. J.; Caprioli, R. M.; Skaar, E. P., The innate immune protein calprotectin promotes *Pseduomonas aeruginosa* and *Staphylococcus aureus* interaction. *Nature Communications* **2016,** *7*, 11951.
42. Palma, M.; Worgall, S.; Quadri, L. E. N., Transcriptome analysis of the *Pseudomonas aeruginosa* response to iron. *Archives of Microbiology* **2003,** *180*, 374-379.
43. Cox, C. D., Iron uptake with ferripyochelin and ferric citrate by *Pseudomonas aeruginosa*. *Journal of Bacteriology* **1980,** *142* (2), 581-587.
44. Ayala-Castro, C.; Saini, A.; Outten, F. W., Fe-S cluster assembly pathways in bacteria. *Microbiology and Molecular Biology Reviews* **2008,** *72*, 110-125.

45. Martin-Mora, D.; Ortega, A.; Reyes-Darias, J. A.; García, V.; López-Farfán, D.; Matilla, M. A.; Krell, T., Identification of a chemoreceptor in *Pseudomonas aeruginosa* that specifically mediates chemotaxis toward α-ketoglutarate. *Frontiers in Microbiology* **2016,** *7*, 1397.
46. Sampedro, I.; Parales, R. E.; Krell, T.; Hill, J. E., *Pseudomonas* chemotaxis. *FEMS Microbiology Reviews* **2015,** *39*, 17-46.
47. Costerton, J. W.; Lewandowski, Z., Microbial biofilms. *Annual Review of Microbiology* **1995,** *49*, 711-745.
48. Heydorn, A.; Nielsen, A. T.; Hentzer, M.; Sternberg, C.; Givskov, M.; Ersbøll, B. K., Quantification of biofilm structures by the novel computer program COMSTAT. *Microbiology* **2000,** *146* (10), 2395-2407.
49. Sauer, K.; Cullen, M. C.; Rickard, A. H.; Zeef, L. A. H.; Davies, D. G.; Gilbert, P., Characterization of nutrient-induced dispersion in *Pseudomonas aeruginosa* PAO1 biofilm. *Journal of Bacteriology* **2004,** *186* (21), 7312-7326.
50. Harmsen, M.; Yang, L.; Pamp, S. J.; Tolker-Nielsen, T., An update on *Pseudomonas aeruginosa* biofilm formation, tolerance, and dispersal. *FEMS Immunology & Medical Microbiology* **2010,** *59*, 253-268.
51. Pamp, S. J.; Tolker-Nielsen, T., Multiple roles of biosurfactants in structural biofilm development by *Pseudomonas aeruginosa*. *Journal of Bacteriology* **2007,** *189*, 2531-2539.
52. Boles, B. R.; Thoendel, M.; Singh, P. K., Rhamnolipids mediate detachment of *Pseudomonas aeruginosa* from biofilm. *Molecular Microbiology* **2005,** *57* (5), 1210-1223.
53. Schooling, S. R.; Charaf, U. K.; Allison, D. G.; Gilbert, P., A role of rhamnolipid in biofilm dispersion. *Biofilms* **2004,** *1* (2), 91-99.
54. Yang, L.; Barken, K. B.; Skindersoe, M. E.; Christensen, A. B.; Givskov, M.; Tolker-Nielsen, T., Effects of iron on DNA release and biofilm development by *Pseudomonas aeruginosa*. *Microbiology* **2007,** *153* (5), 1318-1328.
55. Conrad, R. S.; Wulf, R. G.; Clay, D. L., Effects of carbon sources on antibiotic resistance in *Pseudomonas aeruginosa*. *Antimicrobial Agents and Chemotherapy* **1979,** *15* (1), 59-66.
56. Zhao, W.-H.; Hu, Z.-Q., β-Lactamases identified in clinical isolates of *Pseudomonas aeruginosa*. *Critical Reviews in Microbiology* **2010,** *36* (3), 245-258.
57. Chatterjee, M.; Anju, C. P.; Biswas, L.; Kumar, V. A.; Mohan, C. G.; Biswas, R., Antibiotic resistance in *Pseudomonas aeruginosa* and alternative therapeutic options. *International Journal of Medical Microbiology* **2016,** *306*, 48-58.
58. Liu, Y.; Yang, L.; Molin, S., Synergistic activities of an efflux pump inhibitor and iron chelators against *Pseudomonas aeruginosa* growth and biofilm formation. *Antimicrobial Agents and Chemotherapy* **2010,** *54* (9), 3960-3963.
59. Poole, K.; Krebes, K.; McNally, C.; Neshat, S., Multiple antibiotic resistance in *Pseudomonas aeruginosa*: evidence for involvement of an efflux operon. *Journal of Bacteriology* **1993,** *175* (22), 7363-7372.
60. Langendonk, F. R.; Neil, D. R.; Fothergill, J. L., The building blocks of antimicrobial resistance in *Pseudomonas aeruginosa*: implications for current resistance-breaking therapies. *Frontiers in Cellular and Infection Microbiology* **2021,** *11*, 665759.
61. Macfarlane, E. L. A.; Kwasnicka, A.; Ochs, M. M.; Hancock, R. E. W., PhoP-PhoQ homologues in *Pseudomonas aeruginosa* regulate expression of the outer-membrane protein OprH and polymyxin B resistance. *Molecular Microbiology* **1999,** *34* (2), 305-316.
62. Chevalier, S.; Bouffartigues, E.; Bodilis, J.; Maillot, O.; Lesouhaitier, O.; Feuilloley, M. G. J.; Orange, N.; Dufour, A.; Cornelis, P., Structure, function and regulation of *Pseudomonas aeruginosa* porins. *FEMS Microbiology Reviews* **2017,** *41*, 698-722.
63. Chung, E. S.; Lee, J.-Y.; Rhee, J.-Y.; Ko, K. S., Colistin resistance in *Pseudomonas aeruginosa* that is not linked to *arnB*. *Journal of Medical Microbiology* **2017,** *66*, 833-841.

64. Halder, S.; Yadav, K. K.; Sarkar, R.; Mukherjee, S.; Saha, P.; Haldar, S.; Karmakar, S.; Sen, T., Alteration of Zeta potential and membrane permeability in bacteria: a study with cationic agents. *SpringerPlus* **2015,** *4*, 672.
65. Edrington, T. C.; Kintz, E.; Goldberg, J. B.; Tamm, L. K., Structural basis for the interaction of lipopolysaccharide with outer membrane protein H (OprH) from *Pseudomonas aeruginosa*. *The Journal of Biological Chemistry* **2011,** *286* (45), 39211-39223.
66. Yoshimura, F.; Nikaido, H., Permeability of *Pseudomonas aeruginosa* outer membrane to hydrophilic solutes. *Journal of Bacteriology* **1982,** *152* (2), 636-642.
67. Ude, J.; Tripathi, V.; Buyck, J. M.; Söderholm, S.; Cunrath, O.; Fanous, J.; Claudi, B.; Egli, A.; Schleberger, C.; Hiller, S.; Bumann, D., Outer membrane permeability: antimicrobials and diverse nutrients bypass porins in *Pseudomonas aeruginosa*. *PNAS* **2021,** *118* (31), e2107644118.
68. Xia, Y.; Wang, D.; Pan, X.; Xia, B.; Weng, Y.; Long, Y.; Ren, H.; Zhou, J.; Jin, Y.; Bai, F.; Cheng, Z.; Jin, S.; Wu, W., TpiA is a key metabolic enzyme that affects virulence and resistance to aminoglycoside antibiotics through CrcZ in *Pseudomonas aeruginosa*. *mBio* **2020,** *11* (1), e02079-19.
69. Fléchard, M.; Duchesne, R.; Tahrioui, A.; Bouffartigues, E.; Depayras, S.; Hardouin, J.; Lagy, C.; Maillot, O.; Tortuel, D.; Azuama, C. O.; Clamens, T.; Duclairoir-Poc, C.; Catel-Ferreira, M.; Gicquel, G.; Feuilloley, M.; Lesouhaitier, O.; Heipieper, H.; Groleau, M.-C.; Déziel, E.; Cornelis, P.; Chevalier, S., The absence of SigX results in impaired carbon metabolism and membrane fluidity in *Pseudomonas aeruginosa*. *Scientific Reports* **2018,** *8* (1), 17212.
70. Chevalier, S.; Bouffartigues, E.; Bazire, A.; Tahrioui, A.; Duchesne, R.; Tortuel, D.; Maillot, O.; Clamens, T.; Orange, N.; Feuilloley, M. G. J.; Lesouhaitier, O.; Dufour, A.; Cornelis, P., Extracytoplasmic function sigma factors in *Pseudomonas aeruginosa*. *BBA-Gene Regulatory Mechanisms 1862* **2018**, 706-721.
71. Bouffartigues, E.; Si Hadj Mohand, I.; Maillot, O.; Tortuel, D.; Omnes, J.; David, A.; Tahrioui, A.; Duchesne, R.; Azuama, C. O.; Nusser, M.; Brenner-Weiss, G.; Bazire, A.; Connil, N.; Orange, N.; Feuilloley, M. G. J.; Lesouhaitier, O.; Dufour, A.; Cornelis, P.; Chevalier, S., The temperature-regulation of *Pseudomonas aeruginosa cmaX-cfrX-cmpX* operon reveals an intriguing molecular network involving the sigma factors AlgU and SigX. *Frontiers in Microbiology* **2020,** *11*, 579495.
72. Tortuel, D.; Tahrioui, A.; Rodrigues, S.; Cambronel, M.; Boukerb, A. M.; Maillot, O.; Verdon, J.; Bere, E.; Nusser, M.; Brenner-Weiss, G.; David, A.; Azuama, C. O.; Feuilloley, M. G. J.; Orange, N.; Lesouhaitier, O.; Cornelis, P.; Chevalier, S.; Bouffartigues, E., Activation of the cell wall stress response in *Pseudomonas aeruginosa* infected by a Pf4 phage variant. *Microorganisms* **2020,** *8* (11), :1700.
73. Boechat, A. L.; Kaihami, G. H.; Politi, M. J.; Lépine, F.; Baldini, R. L., A novel role for an ECF sigma factor in fatty acid biosynthesis and membrane fluidity in *Pseudomonas aeruginosa*. *PLOS ONE* **2013,** *8* (12), e84775.
74. Blanka, A.; Schulz, S.; Eckweiler, D.; Franke, R.; Bielecka, A.; Nicolai, T.; Casilag, F.; Düvel, J.; Abraham, W.-R.; Kaever, V.; Häussler, S., Identification of the alternative sigma factor SigX regulon and its implications for *Pseudomonas aeruginosa* pathogenicity. *Journal of bacteriology* **2014,** *196* (2), 345-356.
75. Görke, B.; Stülke, J., Carbon catabolite repression in bacteria: many ways to make the most out of nutrients. *Nature Reviews Microbiology* **2008,** *6*, 613-624.

For TOC Only

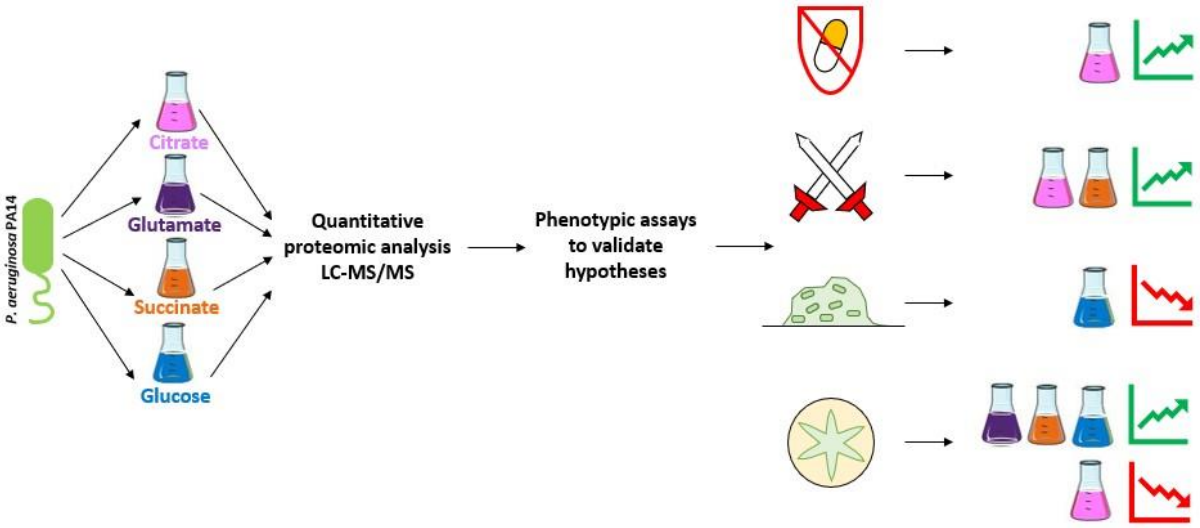
P. aeruginosa PA14
Citrate
Glutamate
Succinate
Glucose
Quantitative proteomic analysis LC-MS/MS
Phenotypic assays to validate hypotheses